INFRARED SIGNATURES OF INTERACTIONS BETWEEN MOLECULES AND FREE CHARGE CARRIERS IN NANOSTRUCTURES

Annemarie Pucci,

Kirchhoff Institute for Physics and Centre of Advanced Materials of the University of Heidelberg and InnovationLab Heidelberg

iL INNOVATION LAB thinking works

CAM CENTRE FOR ADVANCED MATERIALS

CONTENTS

LOCALIZED SURFACE PLASMON POLARITONS

The free electron gas in a particle has some similarities to water in a swimming pool: In plasmonics we consider the electron gas as incompressible.
External fields can excite waves (pressure waves / em waves). Boundaries determine standing wave pattern.

Dipole-like excitations as oscillation of the free electron gas in a container.

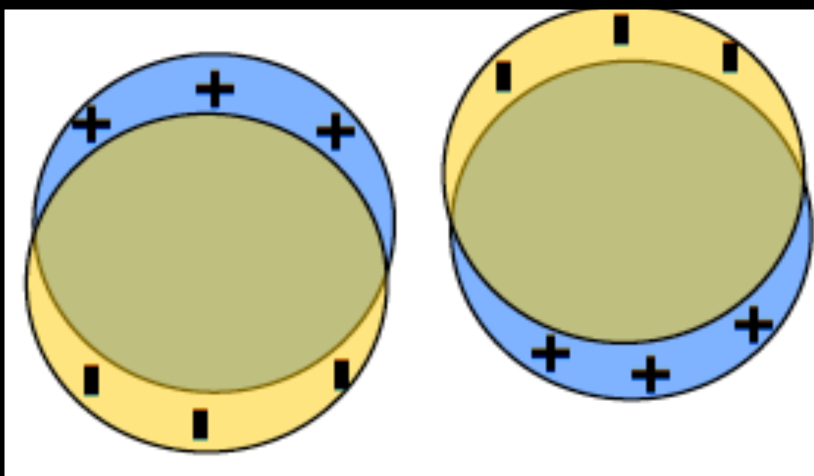

The fundamental (lowest order) excitation.

www.youtube.com

LSPP AND PARTICLE SHAPE

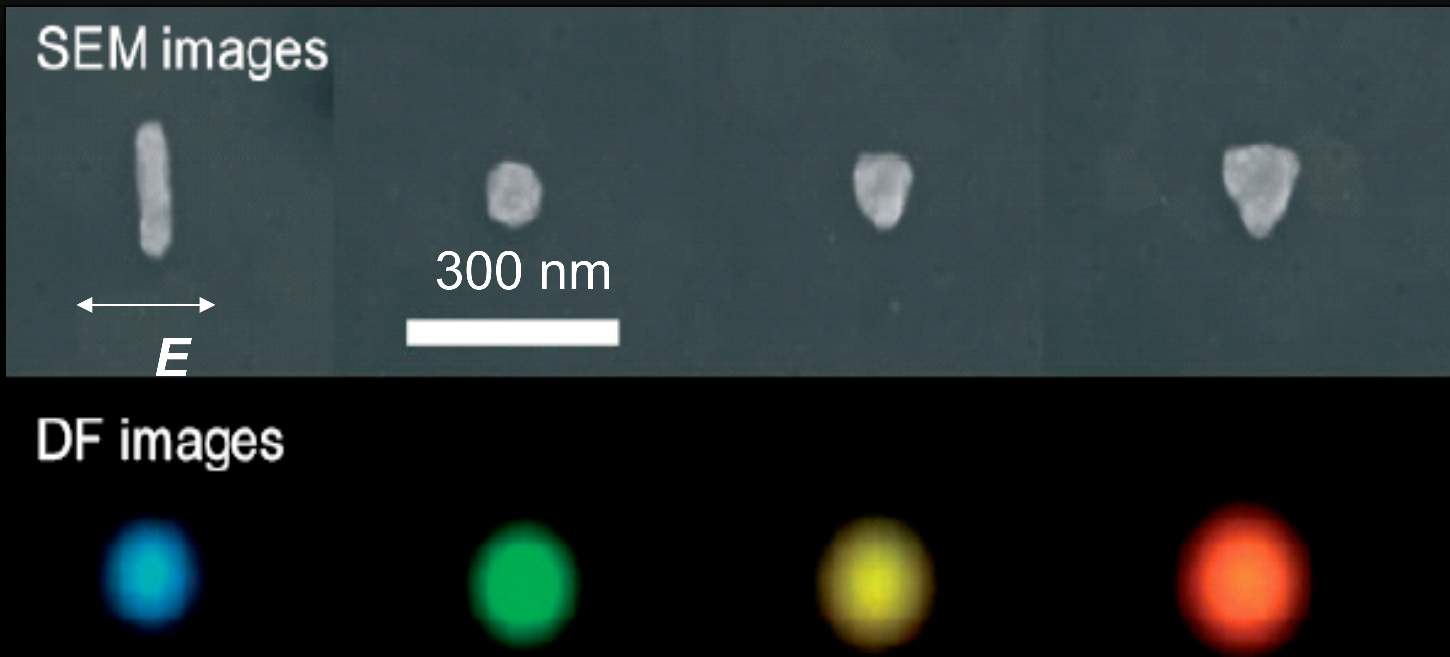

Gold nanoparticles (30 nm height) on glass, dark field mode of the optical microscope

Murray, W. and Barnes, W. (2007), Plasmonic Materials. Advanced Materials, 19: 3771–3782

LSPP of nanowires

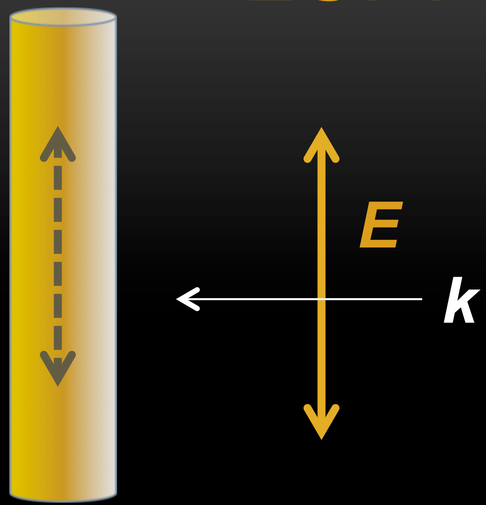

Excitation of a plasmonic dipole oscillation by light polarized parallel to the wire. Standing waves of longitudinal charge oscillation can be excited.

Because $L \approx \lambda$, light scattering is important!

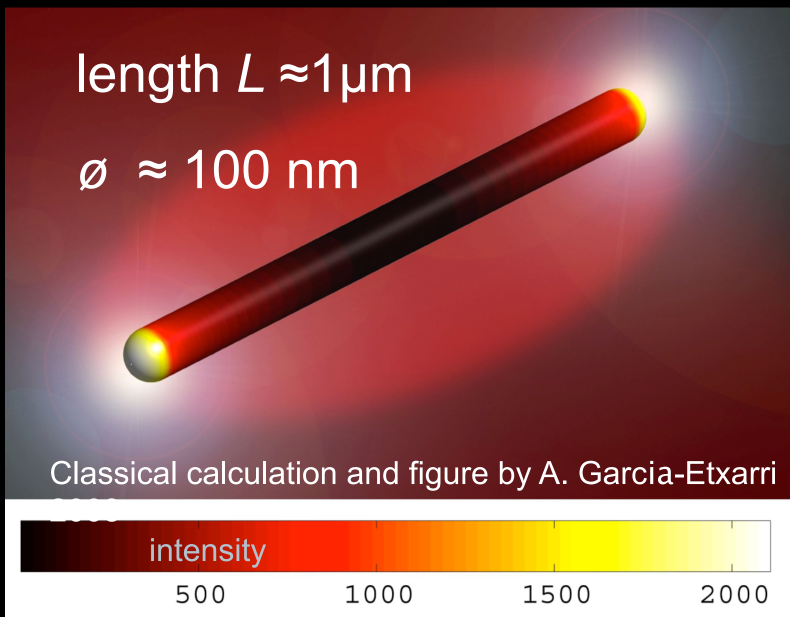

Strong nearfield-intensity enhancement at the nanowire apex

F. Neubrech et al., Phys. Rev. Lett. 101, 157403 (2008)

Plasmon polaritons on a metal cylinder

plot for electrostatic limit $(c \to \infty)$

diameter ρ_0

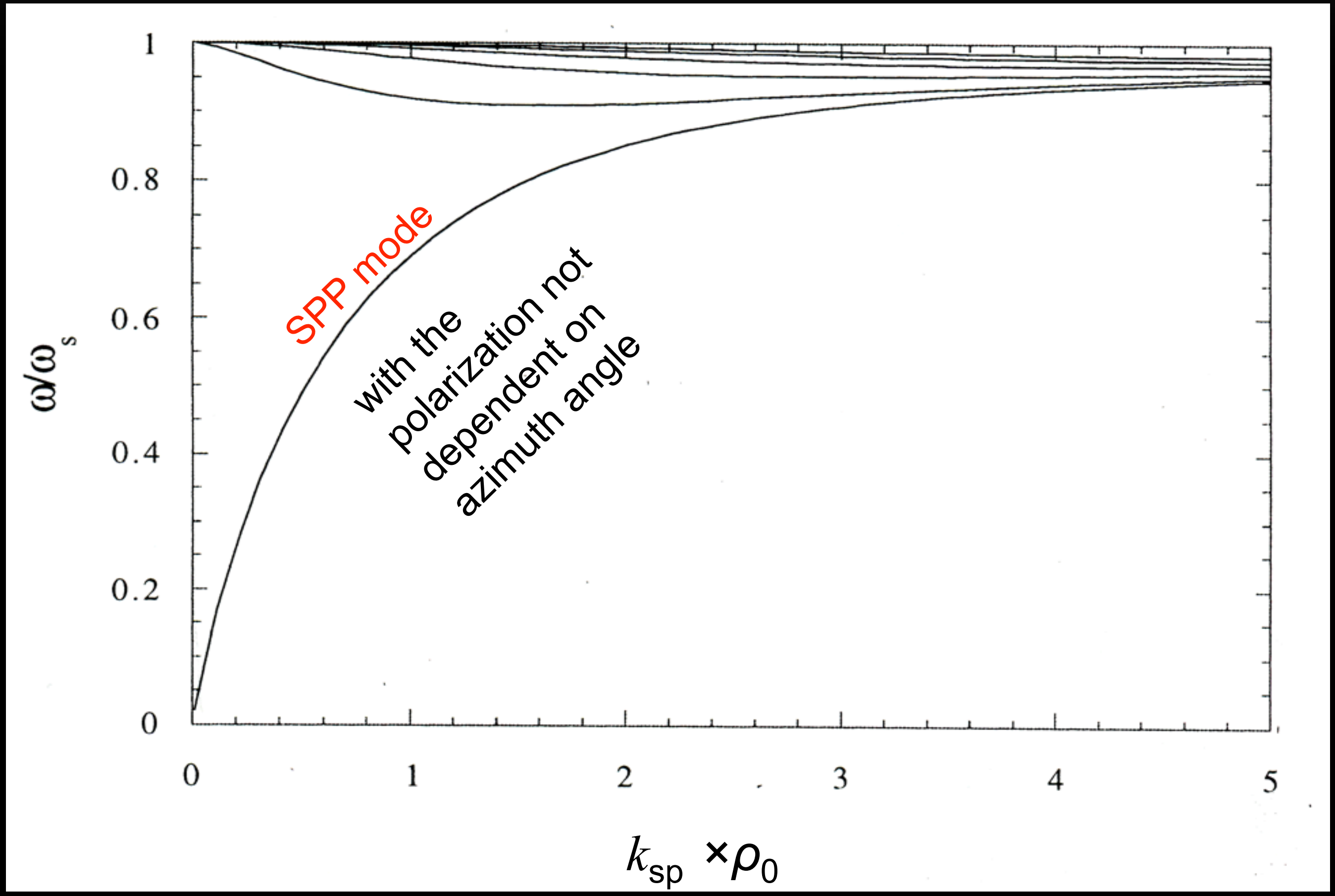

B. E. Sernelius „Surface modes in physics“, Wiley VCH 2001.

Standing wave -plasmon polaritons on a finite metal cylinder

plot for electrostatic limit

diameter ρ_0

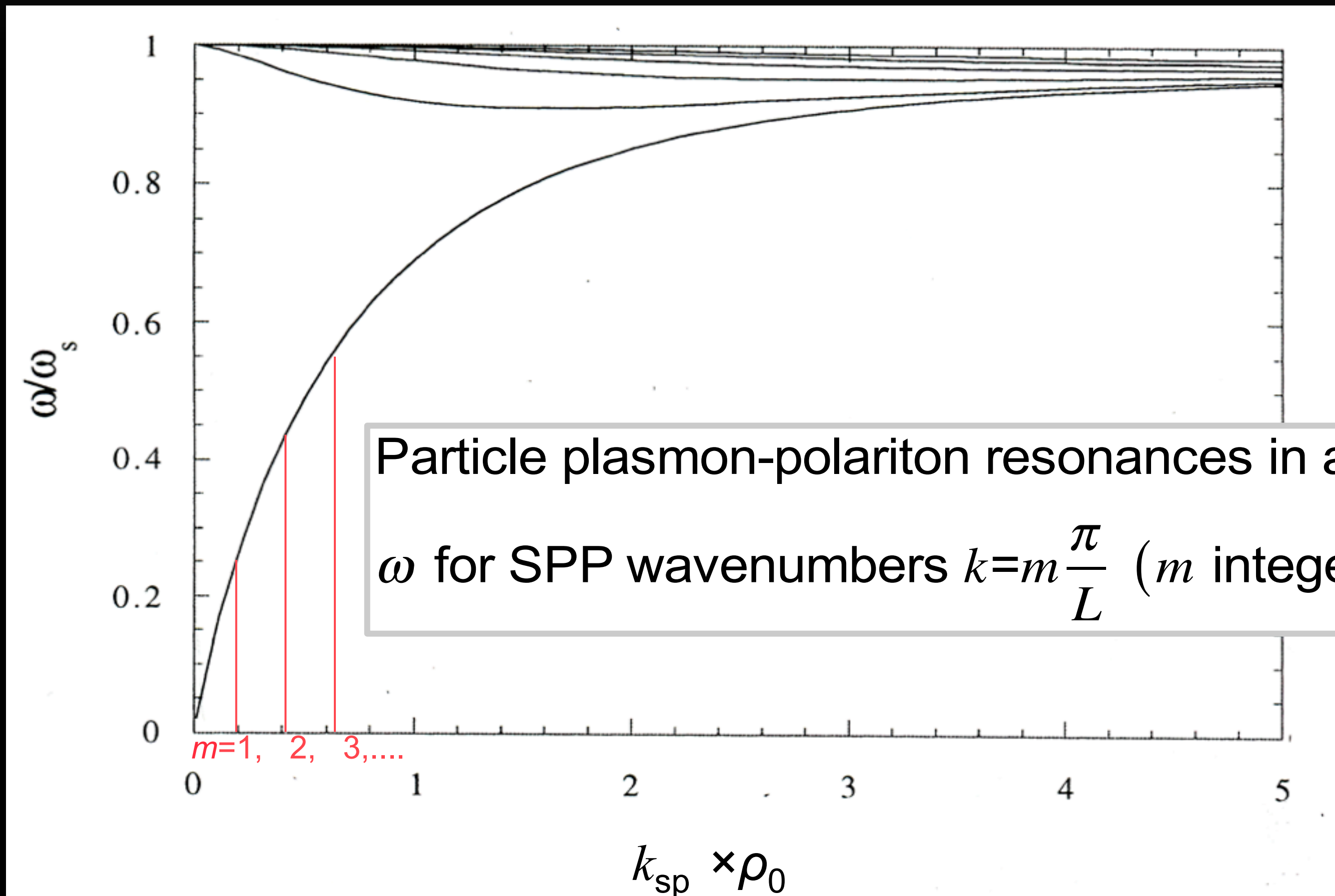

Particle plasmon-polariton resonances in a finite rod:

ω for SPP wavenumbers $k = m\dfrac{\pi}{L}$ $(m$ integer$)$

B. E. Sernelius „Surface modes in physics“, Wiley VCH 2001.

Charge oscillation modes

Examples of surface charge (ρ) oscillation patterns of modes in a nanorod with long axis in *x*-direction.

(J. Aizpurua, et al., Phys. Rev B 2005)

Standing waves of longitudinal charge oscillation $\omega(q)$ are formed in the particle's penetration depth, for m=1, SPP wavelength λ_{LSPP} =2L.

$\omega_{\text{res}} \approx C \cdot \frac{\pi}{L}$ (linear range of dispersion),

LSPP wavenumber $q_{\text{LSPP}} = \frac{\pi}{L} m$

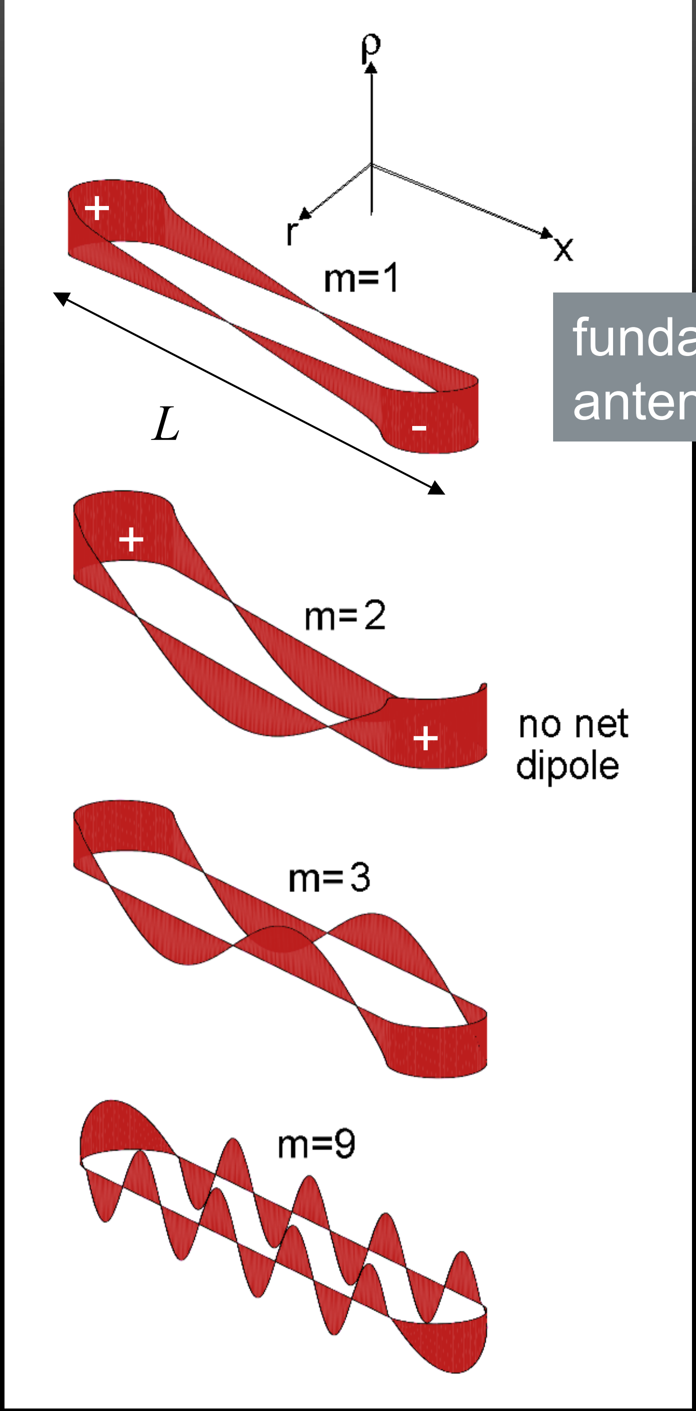

fundamental antenna mode

no net dipole

LITHOGRAPHIC GOLD NANOWIRES

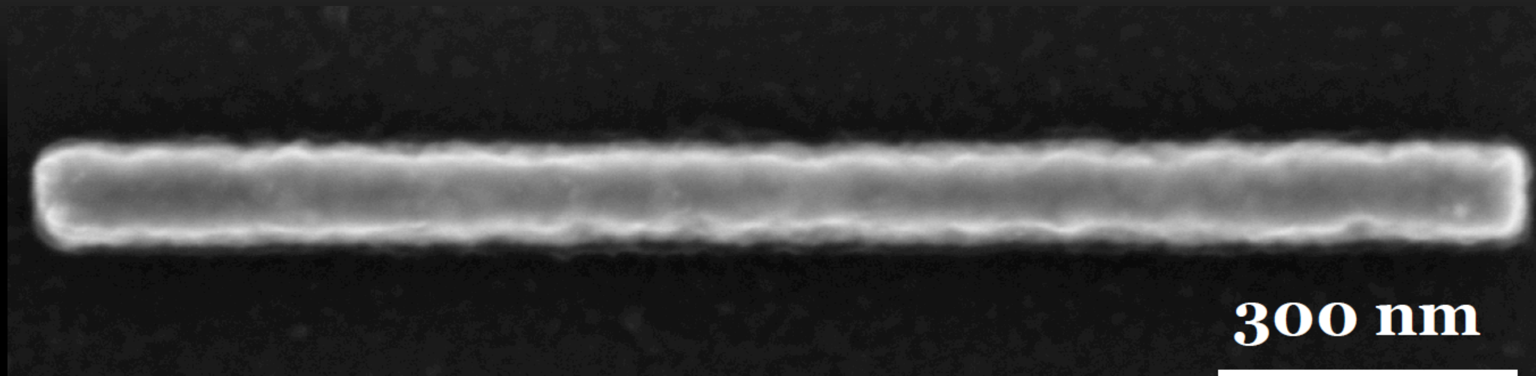

SEM of a typical electron-lithographically (EBL) produced gold antenna (on silicon wafer with natural oxide, 10 nm Ti adhesion layer between gold and silicon oxide).

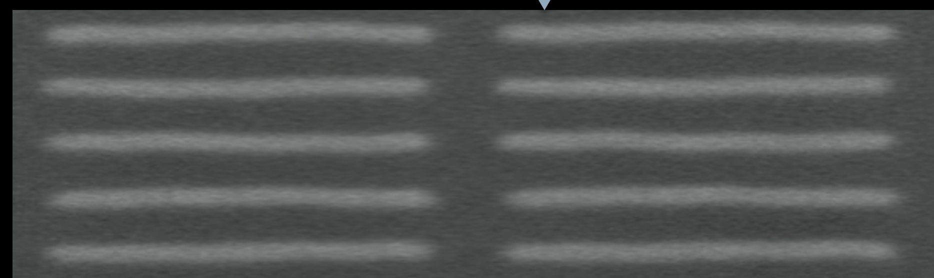

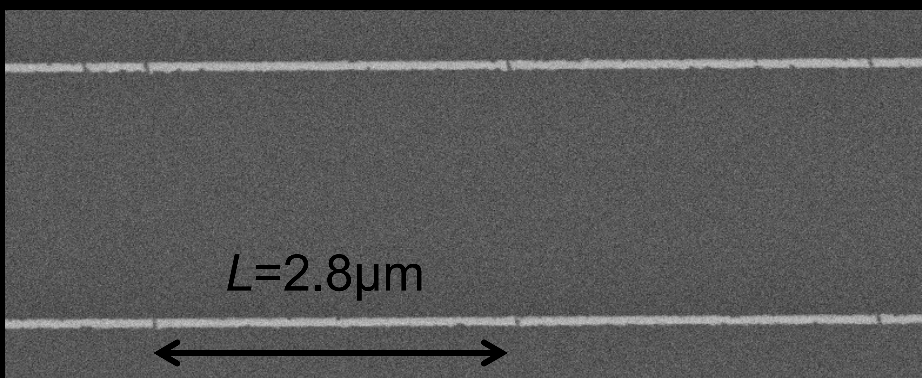

Array of gold antennas on CaF_2 (2014)

A. Hasenkampf et al., Optics Express 23, 5670 (2015).

EXTINCTION CROSS SECTIONS

$$\sigma_{ext} = \sigma_{sca} + \sigma_{abs}$$

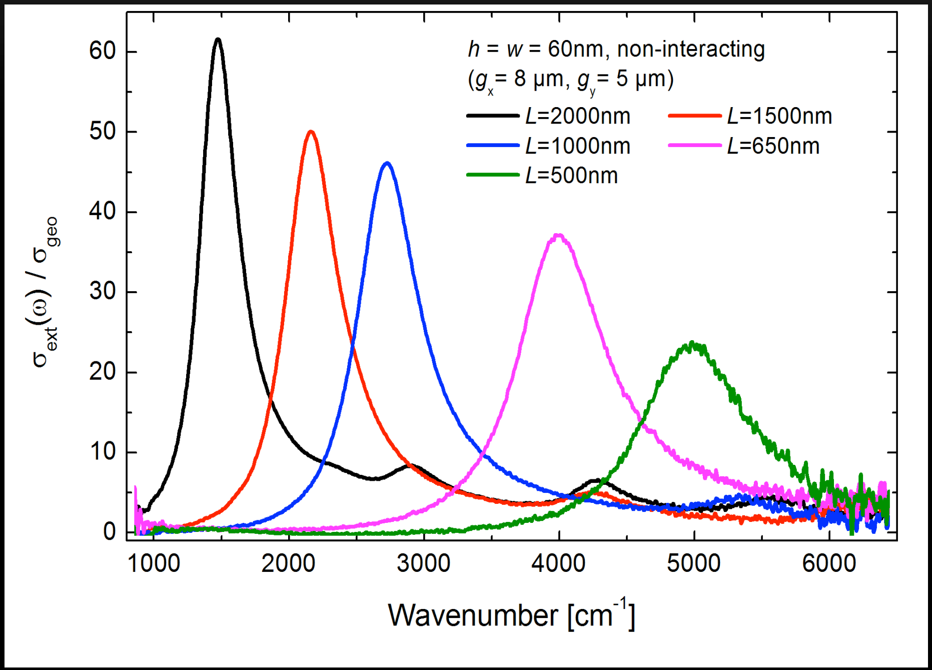

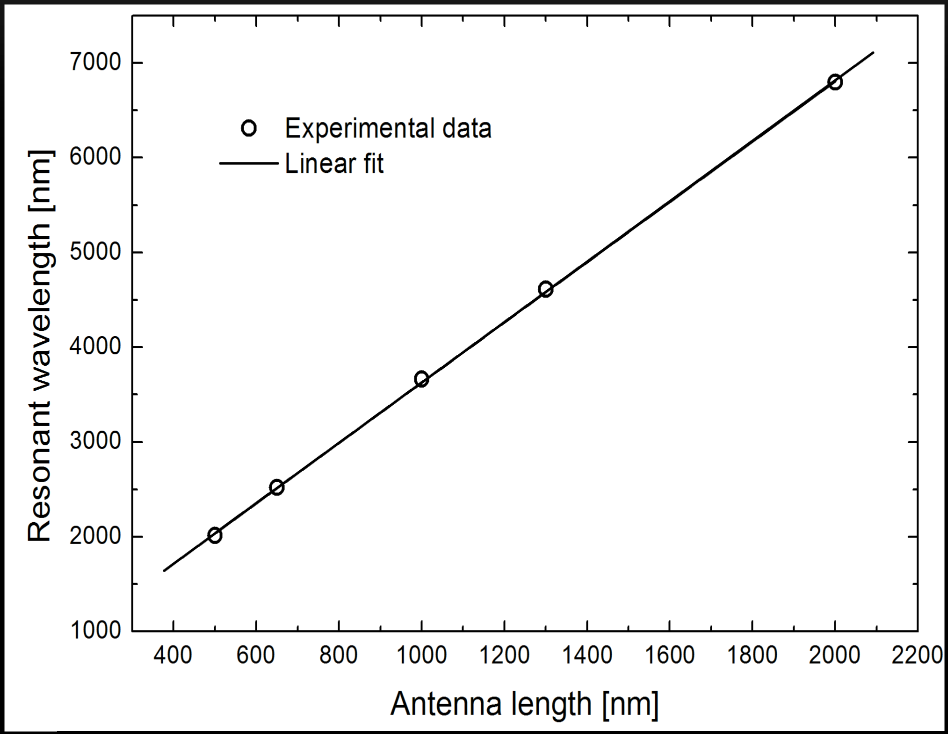

Experimental extinction cross-section (normalized to the geometrical one) of gold nanoantennas with different lengths *L* on a CaF_2 substrate, normal incidence of light with an electrical field vector parallel to the long antenna axis. D. Weber et al., Opt. Mater. Express 1,1301 (2011)

Resonance photon wavelength λ_{res} as extracted from the spectra shown left. The linear relation

$\lambda_{res} = 3.178\, L$ [nm] + 451nm

gives a perfect fit to the data.

RELATIVE IR TRANSMITTANCE* SPECTROSCOPY - SURFACE SENSITIVITY BY CAREFUL REFERENCING

- transmittance at normal incidence
- ultrathin films, nano-particles
- transparent substrate

$d << \lambda / n_{\text{film}}$

relative transmittance

$$T_{\text{rel}} = \frac{T_{\text{film/substrate}}}{T_{\text{substrate}}} \approx 1 - \frac{2 \cdot d \cdot \omega \cdot \text{Im}\varepsilon_{\text{II film}}(\omega)}{c \cdot (1 + n_{\text{substrate}})}$$

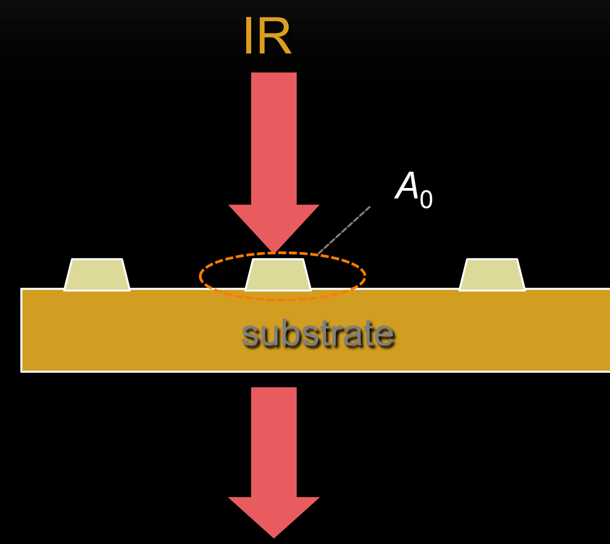

Extinction cross-section σ_{ext} of a nanoparticle

Conductivity measurement without electrical contacts or $\text{Im}\varepsilon_{\text{eff}}(\omega)$ for island films

- For single nanoparticles on a substrate in the focal area A_f:

$$\sigma_{\text{ext}} = A_0 \ (1 - T_{\text{rel}}) \ \cdot (n_{\text{substrate}} + \ 1) \ / \, 2 n_{\text{eff}}$$

*analogous approximations and referencing for other measurement geometries

EXTINCTION

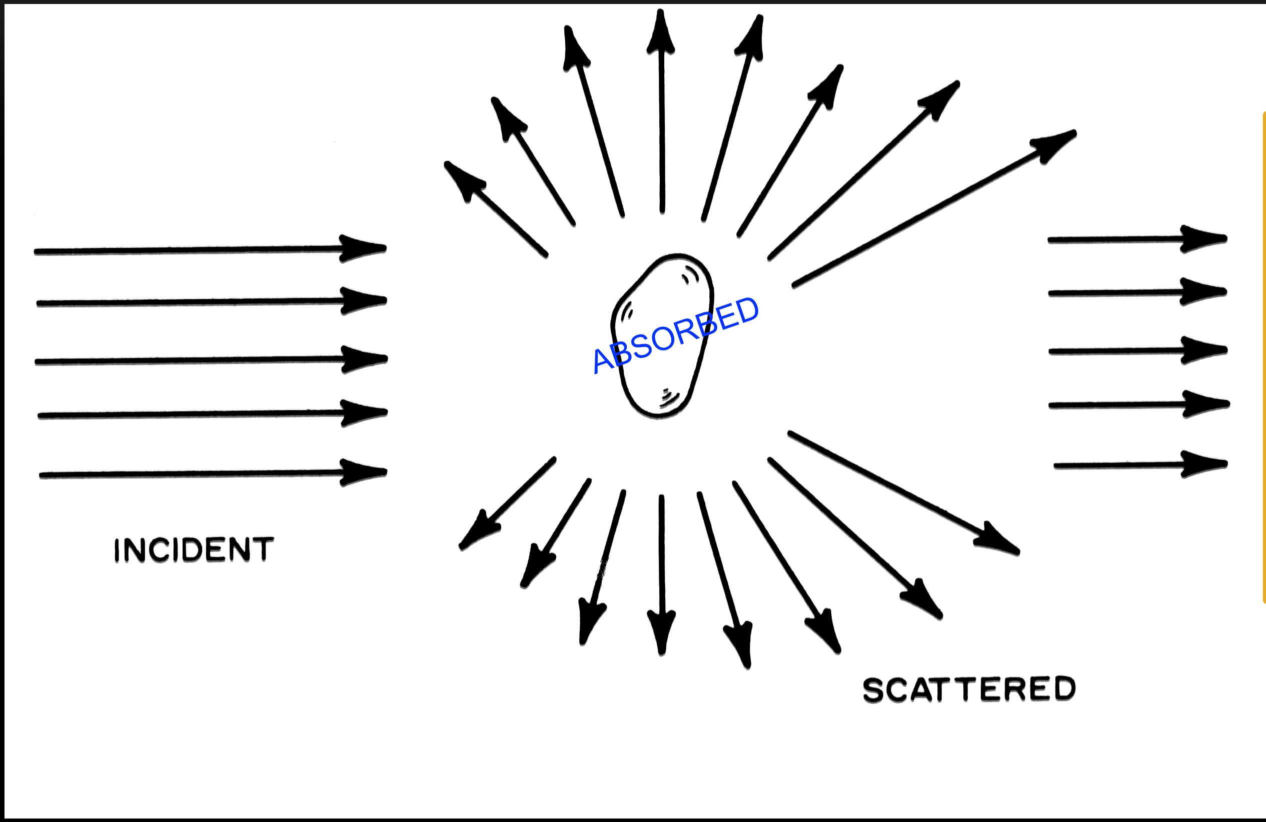

Transmitted intensity, lowered by absorption + scattering = extinction.

absorption $\propto L / \lambda$,

scattering $\propto L^4 / \lambda^4$

after C.F. Bohren and D.R. Huffman, "Absorption and Scattering by Small Particles", Wiley &Sons 1983

QUASISTATIC DESCRIPTION WITH RADIATION-DAMPING CORRECTION FOR A DRUDE-TYPE METAL

J. Vogt et al., Encyclopedia of Nanotechnology 2015, DOI 10.1007/ 978-94-007-6178-0_100977-1, T. Neuman, C. Huck, et al., J. Phys. Chem. C 119, 26652 (2015).

$$\varepsilon(\omega) = \varepsilon_\infty - \frac{\omega_p^2}{\omega(\omega + i\omega_\tau)}$$

$$\sigma_{sca} = \omega_p^2 \frac{VR}{n_{host}c} \frac{\omega^4 T_L}{\left[(\omega_{res}^2 - \omega^2)^2 + \omega^2(\omega_\tau + \omega^2 T_L)^2\right]}$$

$$\sigma_{abs} = \omega_p^2 \frac{VR}{n_{host}c} \frac{\omega^2 \omega_\tau}{\left[(\omega_{res}^2 - \omega^2)^2 + \omega^2(\omega_\tau + \omega^2 T_L)^2\right]}$$

Larmor time parameter $T_L = VRn_{host}\,\omega_p^2/(6\pi c^3)$, local field ratio R.*

*W. T. Doyle, J. Opt. Soc. Am. A. 2, 1031(1985)

GOLD IN THE IR, VARIOUS ELECTRONIC SCATTERING

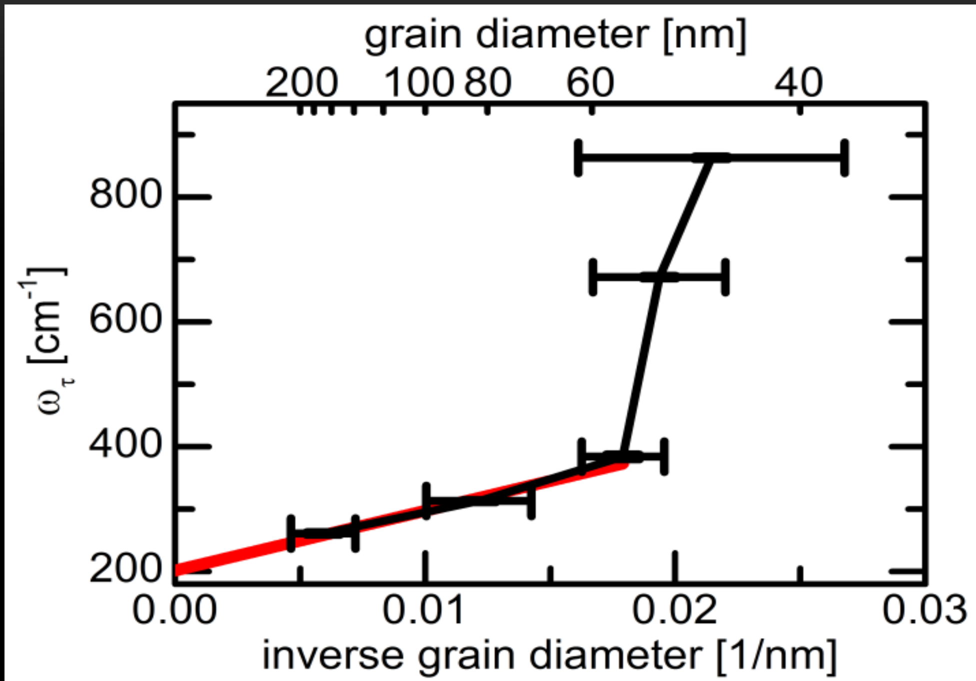

Scattering rates ω_τ for various gold films from IR ellipsometry plotted versus the inverse diameter of grains on the surface (from AFM).

J. Trollmann and A. Pucci, J. Phys. Chem. C 118, 15011 (2014).

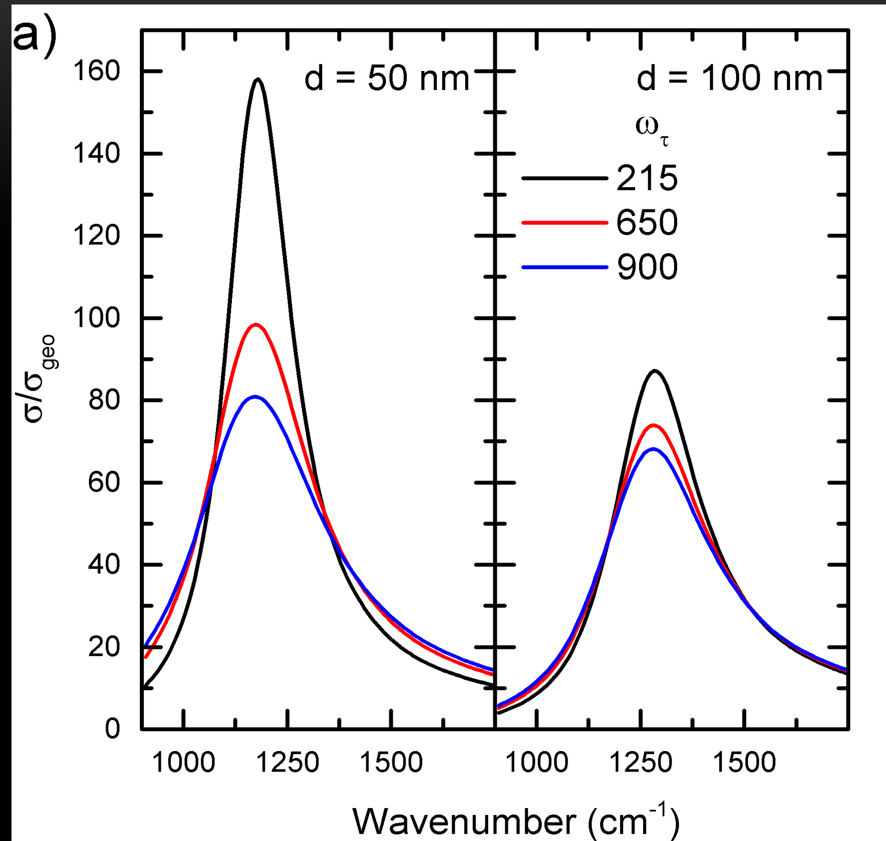

FDTD simulations of extinction for various electronic scattering rates

T. Neuman, C. Huck, et al., J. Phys. Chem. C 119, 26652 (2015).

Example: Pb nanorods on Si(557) - Morphology by AFM

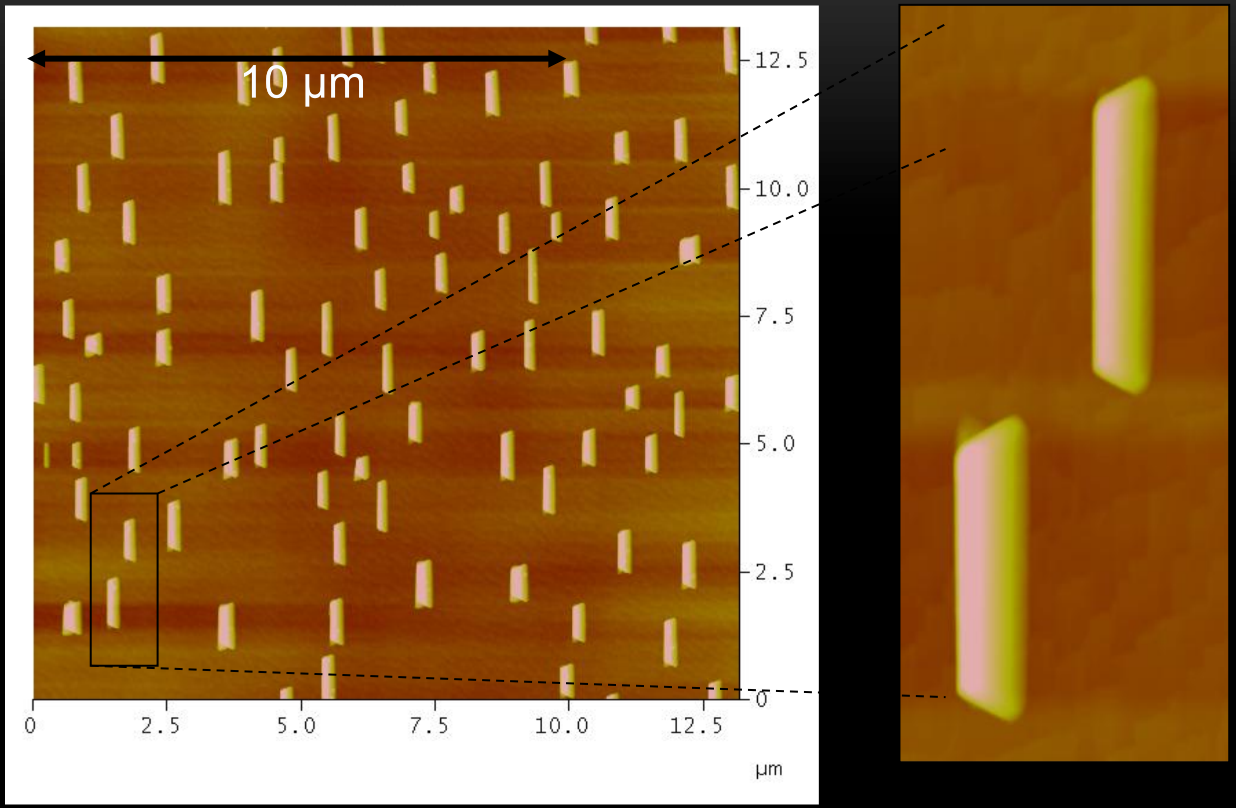

Growth at RT,
10 ML Pb

single-crystalline nanowires with aspect ratio > 3

(Morphology controlled by substrate quality, temperature, Pb flux)

H. V. Chung et al, SPIE Vol. 7394, 73941E (2009)

FUNDAMENTAL PLASMONIC RESONANCE OF LEAD NANORODS ON SI(557)

E II steps

Development with temperature

Average Pb coverage	Length (nm)	Width (nm)	Height (nm)
2 ML	170 ± 30	30 ± 6	5 ± 1
3 ML	585 ± 20	90 ± 6	15 ± 1
5 ML			
10 ML	1126 ± 100	144 ± 12	24 ± 2

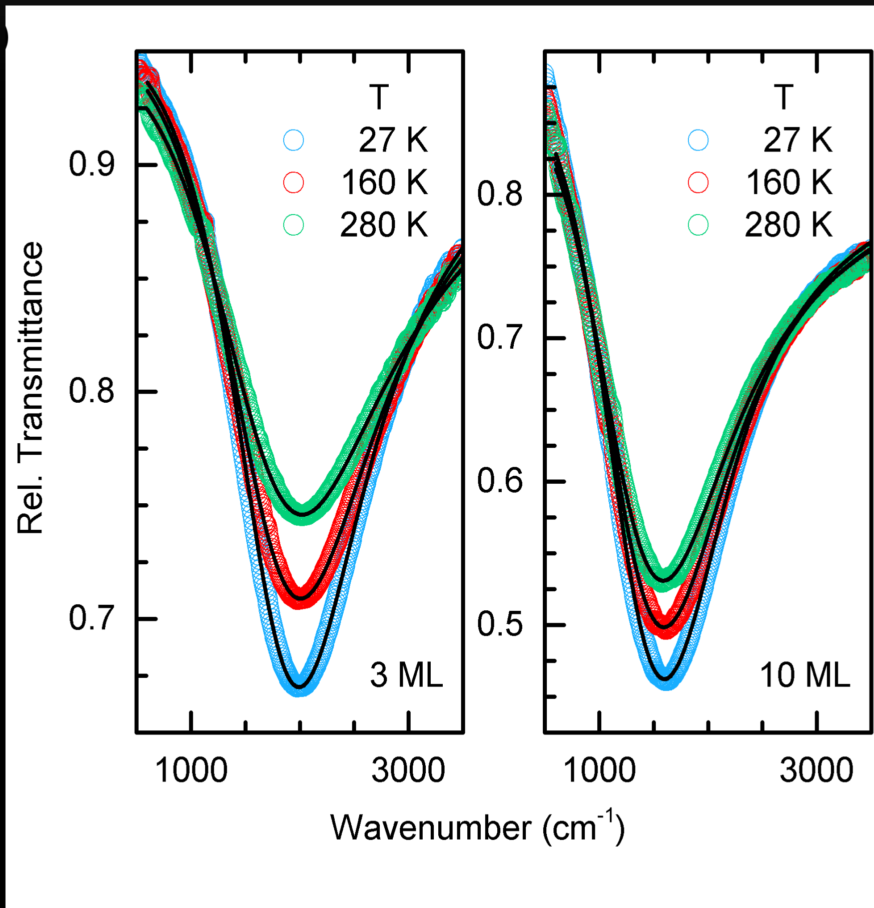

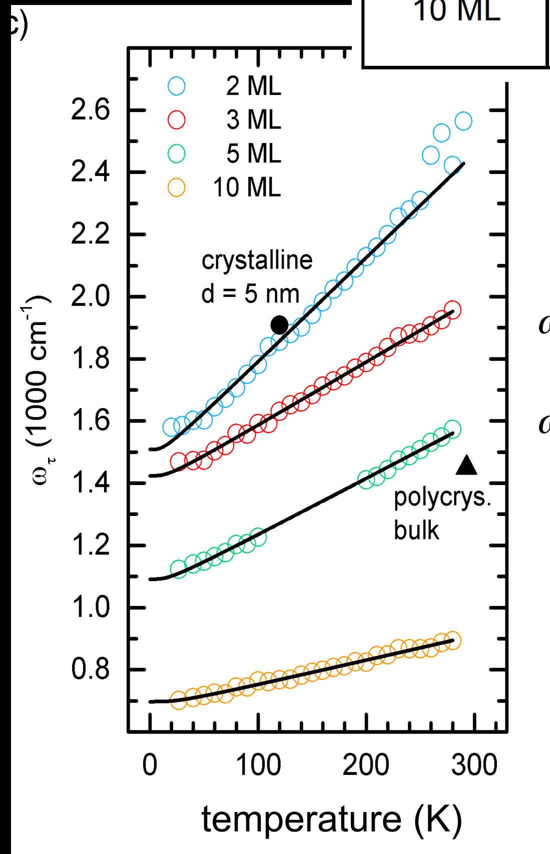

$$\omega_\tau = \omega_{\tau p}(T) + \left[\omega_{\tau s} + \omega_{\tau d}\right],$$

$$\omega_{\tau p} = \frac{1}{\tau_0}\left[\frac{2}{5} + 4\left(\frac{T}{\theta_D}\right)^5 \int_0^{\theta_D/T} \frac{z^4}{e^z - 1} dz\right]$$

as fit function

J. Vogt, Chung Vu Hoang, C. Huck, F. Neubrech, A. Pucci, J Phys. Chem C 120 (2016) 19302.

ANTENNA SIZE FOR MAXIMUM NEAR-FIELD ENHANCEMENT

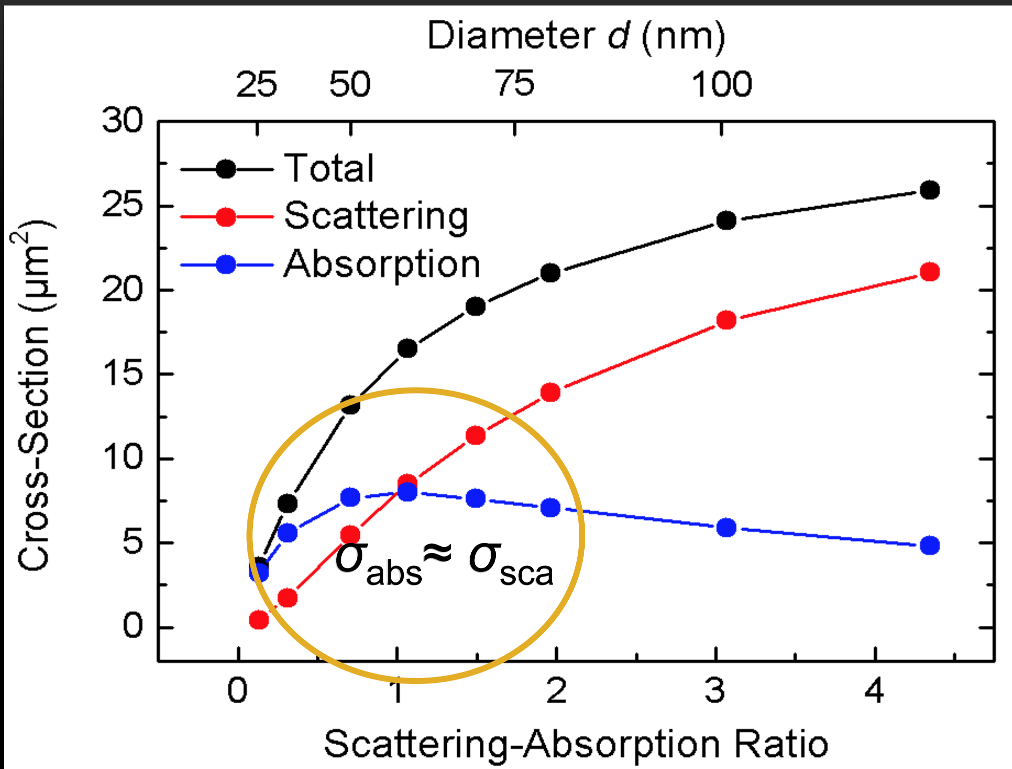

$$\sigma_{abs} = \sigma_{sca} \Leftrightarrow$$

maximum integrated near-field intensity

$$\sigma_{abs}\left(\omega = \omega_{res}\right) = \sigma_{sca}\left(\omega = \omega_{res}\right)$$

$$\Rightarrow \omega_{res}^2 T_L = \omega_{rad} = \omega_\tau ,$$

$\Rightarrow \sigma_{abs}\left(\omega = \omega_{res}\right)$ is maximum regarding the change in antenna volume (or length or diameter)

Resonance cross sections versus scattering-absorption ratio (diameter) for gold antennas (resonance at 1250 cm^{-1}). FDTD simulations with Palik's data for gold.

T. J. Seok, Nano Lett. 11, 2606 (2011).

T. Neuman, C. Huck, et al., J. Phys. Chem. C 119, 26652 (2015).

IR SPECTRA AND FIT RESULTS FOR DAMPING

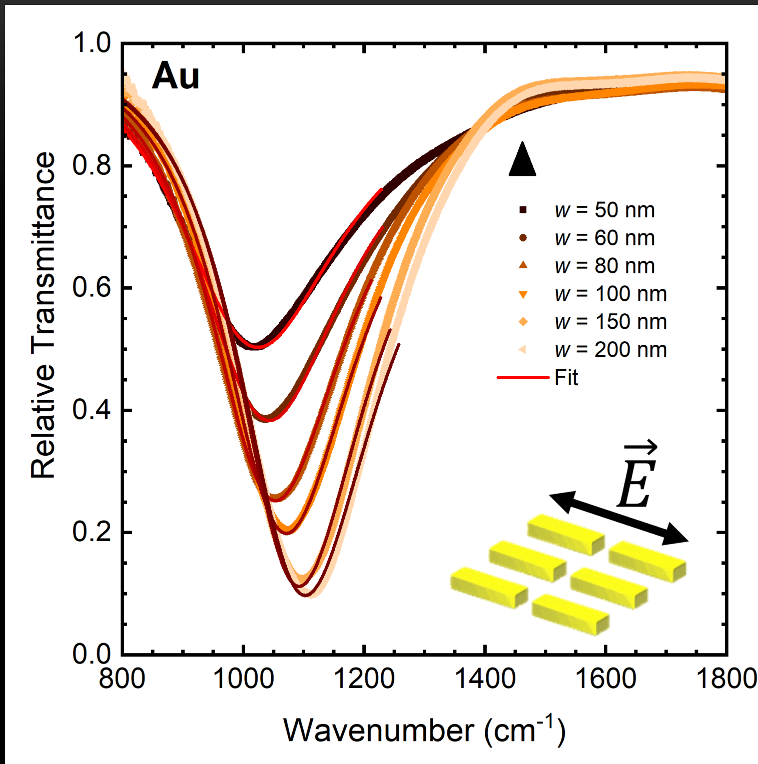

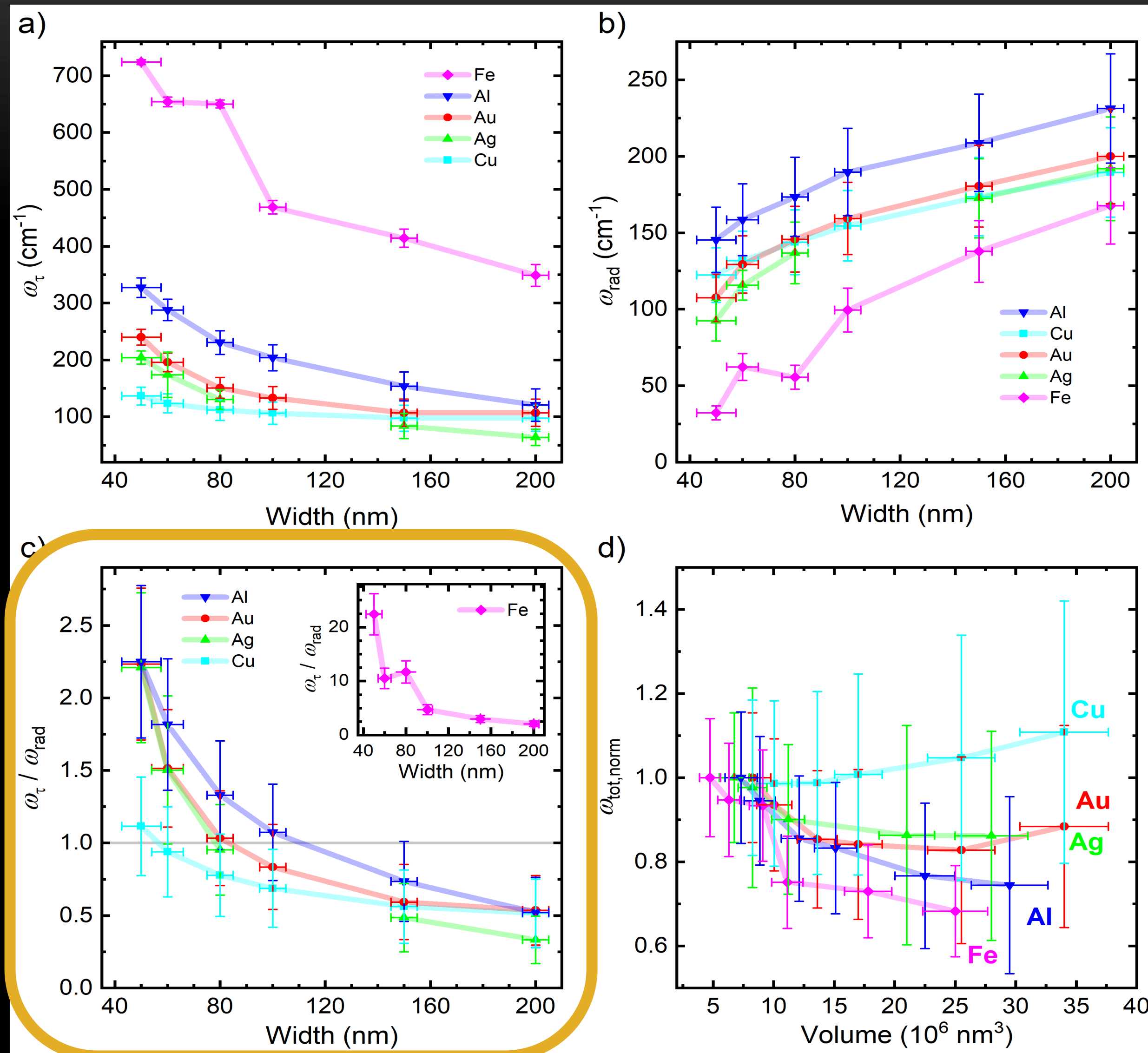

M. Tzschoppe et al., J. Phys. Chem. C 122,15678 (2018)

SEIRA ON VARIOUS ANTENNAS

M. Tzschoppe et al., J. Phys. Chem. C 122,15678 (2018)

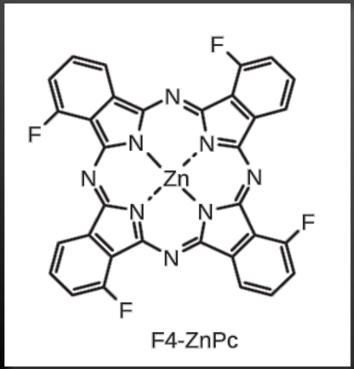

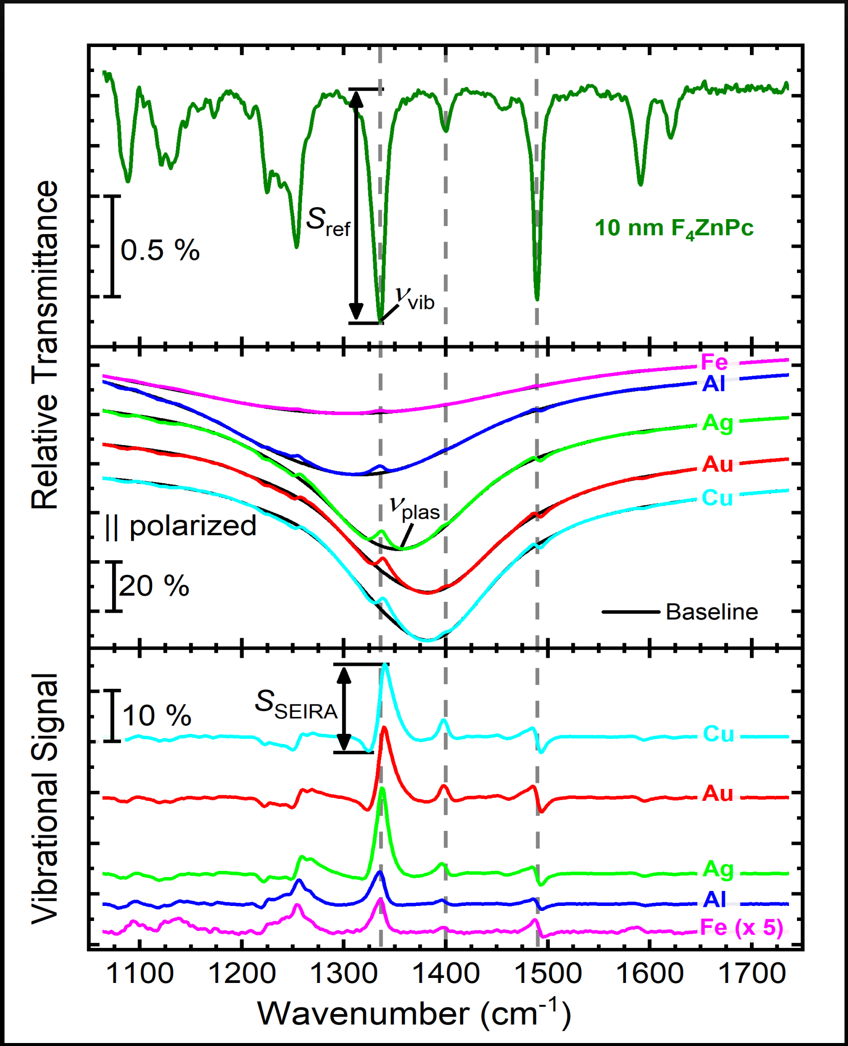

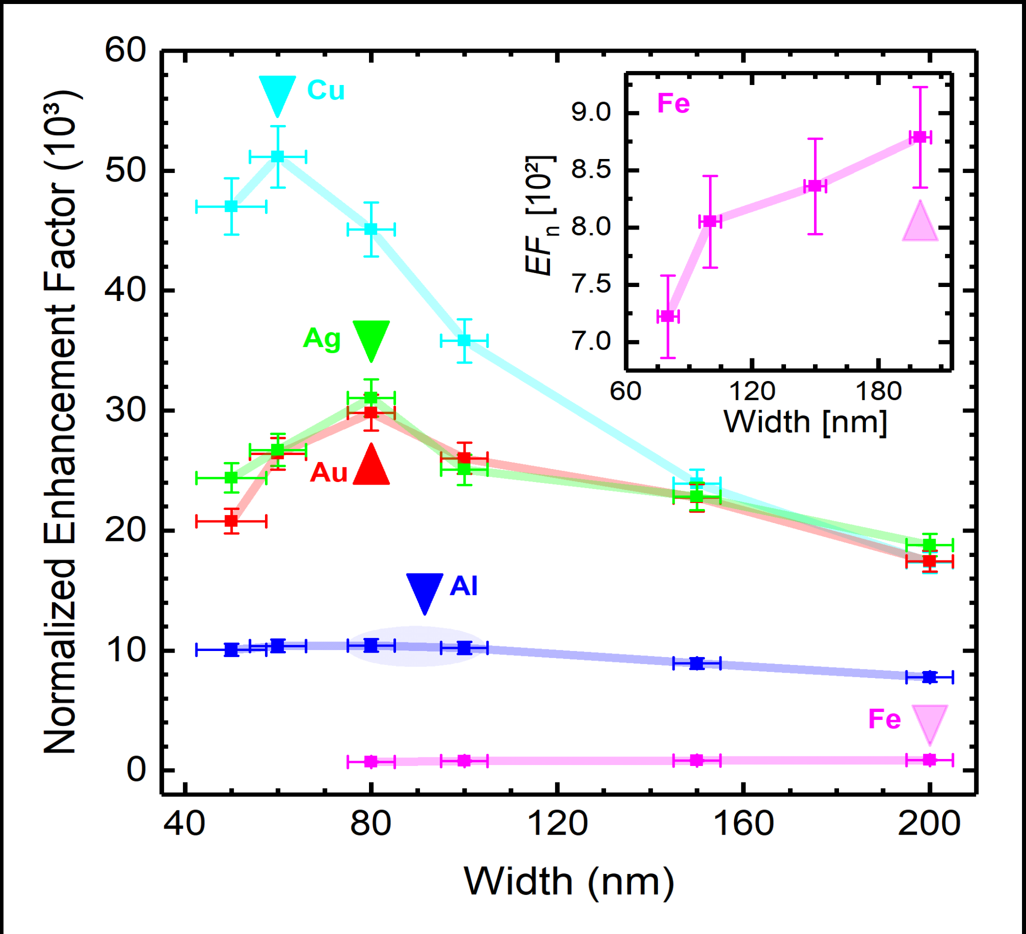

PLASMON-VIBRATION COUPLING AS A FANO EFFECT- SEIRA WITH PLASMONIC RESONANCES

F. Neubrech et al., Phys. Rev. Lett. 101, 157403 (2008)

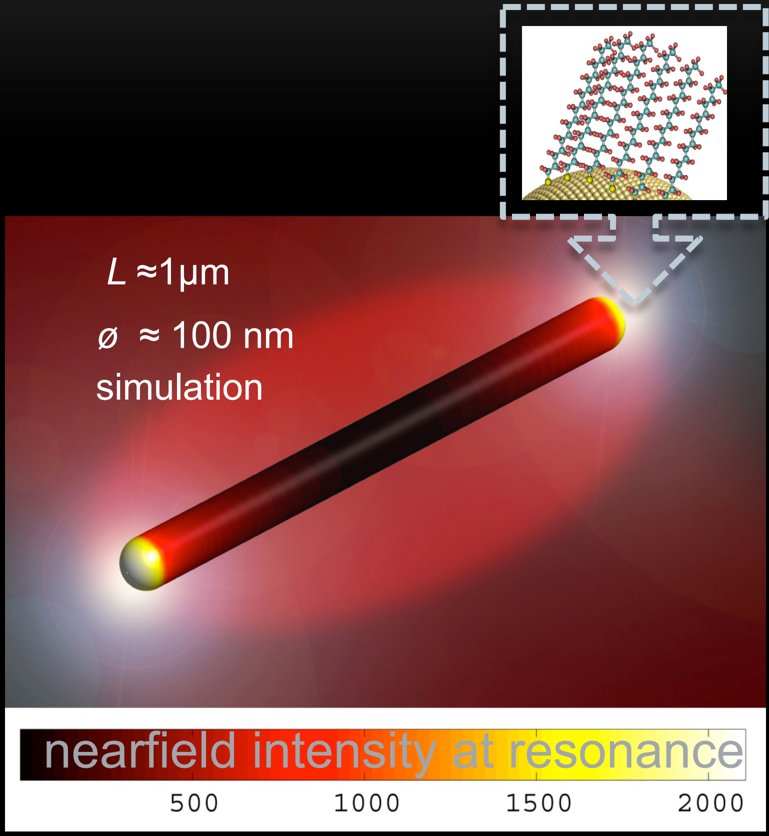

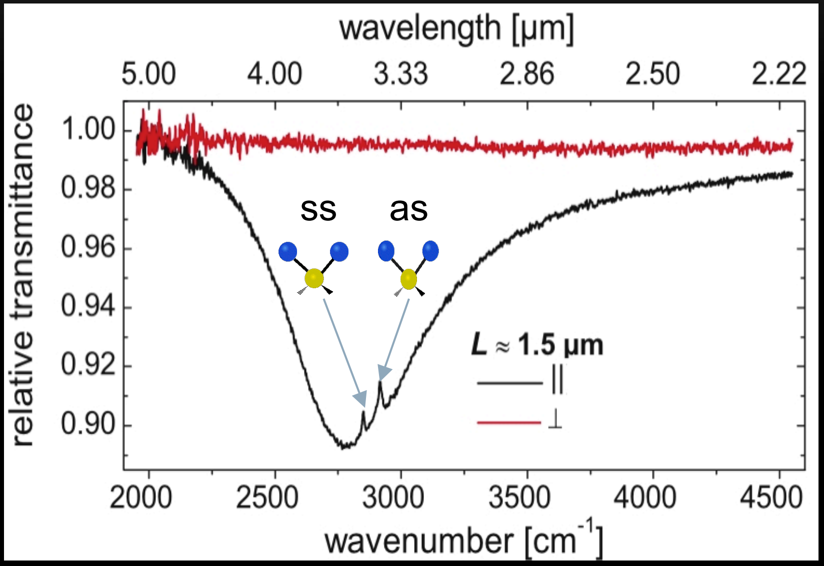

At resonance, the nearfield intensity at the tips is at least by two to three orders of magnitude enhanced

Vibration signals with 1% contrast from one ML octadecanthiole (ODT) molecules on the resonance background of a single antenna corresponds to an increase of extinction.

Signals from ≈1 attomol ODT molecules on the two tip ends of the wire! Vibrational cross section ca. 500 000 times enhanced.

The Fano effect leads to asymmetric lines or even "anti-absorption"

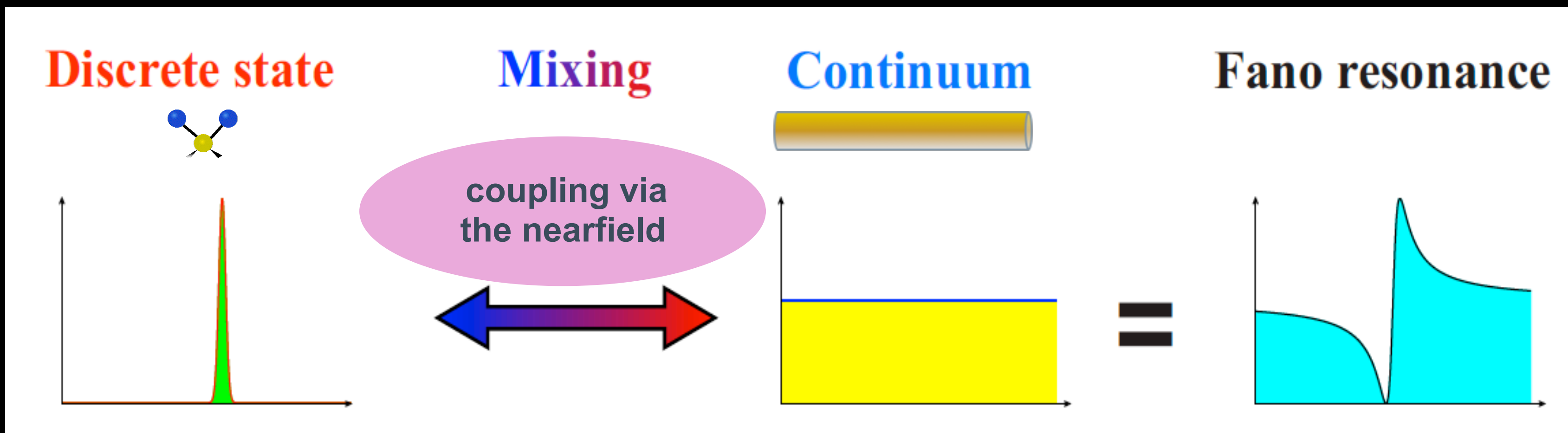

After A. E. Miroshnichenko et al., REVIEWS OF MODERN PHYSICS 82, 2257(2010).

SEIRA OF A LAYER OF ORGANIC MOLECULES

Array on CaF_2 (IIT Genova), *L* ca. 1500 nm, *h*=*w*=60nm, g_x= 50 nm

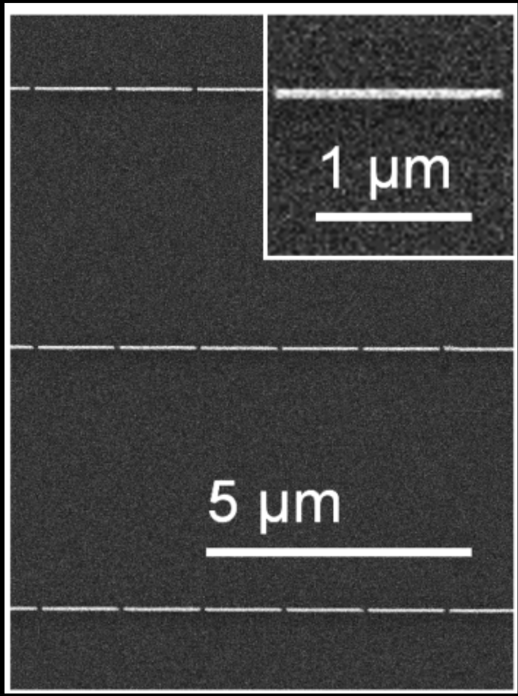

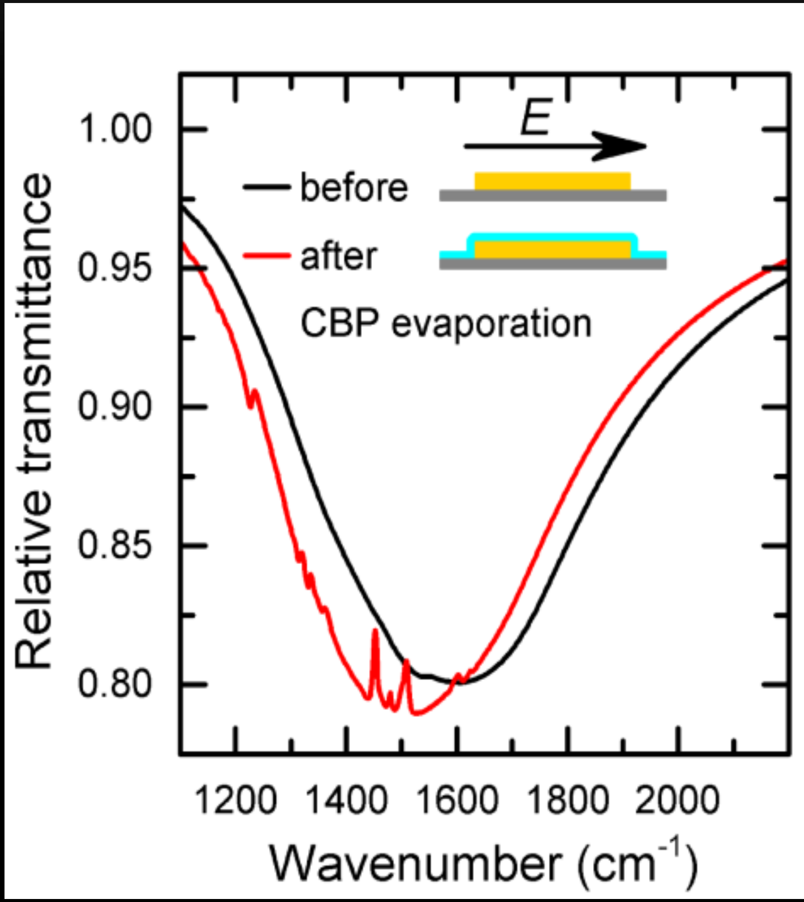

5 nm 4,4-N,N-dicarbazole-biphenyl (CBP)

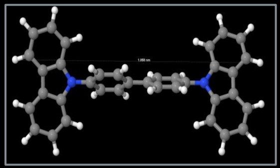

J. Vogt et al. Phys. Chem. Chem. Phys. 17 (2015), 21169-21175.

SEIRA : FREQUENCY TUNING, FANO-LINE SHAPE

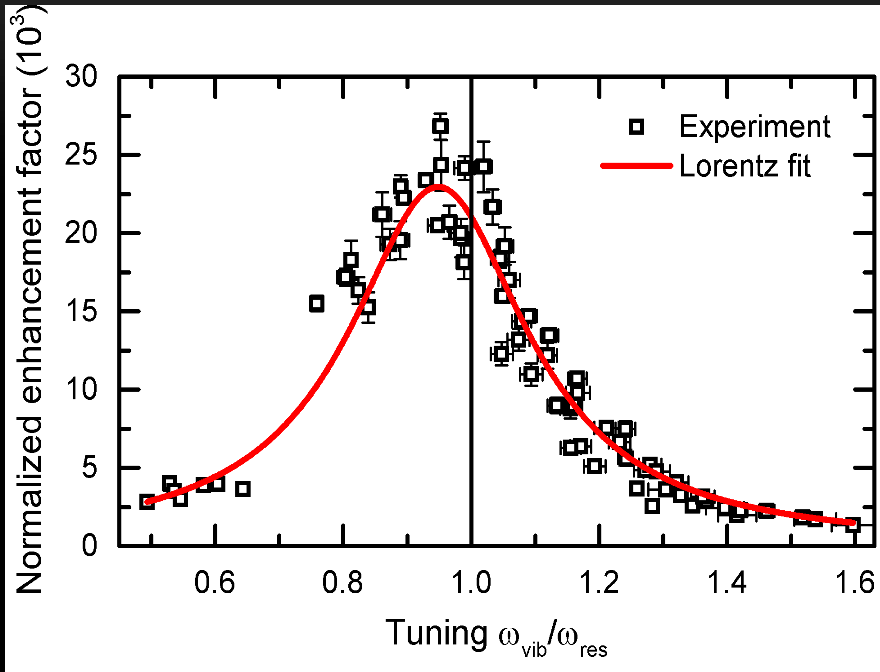

$$f(\varepsilon)=\frac{(q+\varepsilon)^2}{(1+\varepsilon^2)},\ \varepsilon=2(\omega-\omega_{\mathrm{vib}})/\Gamma$$

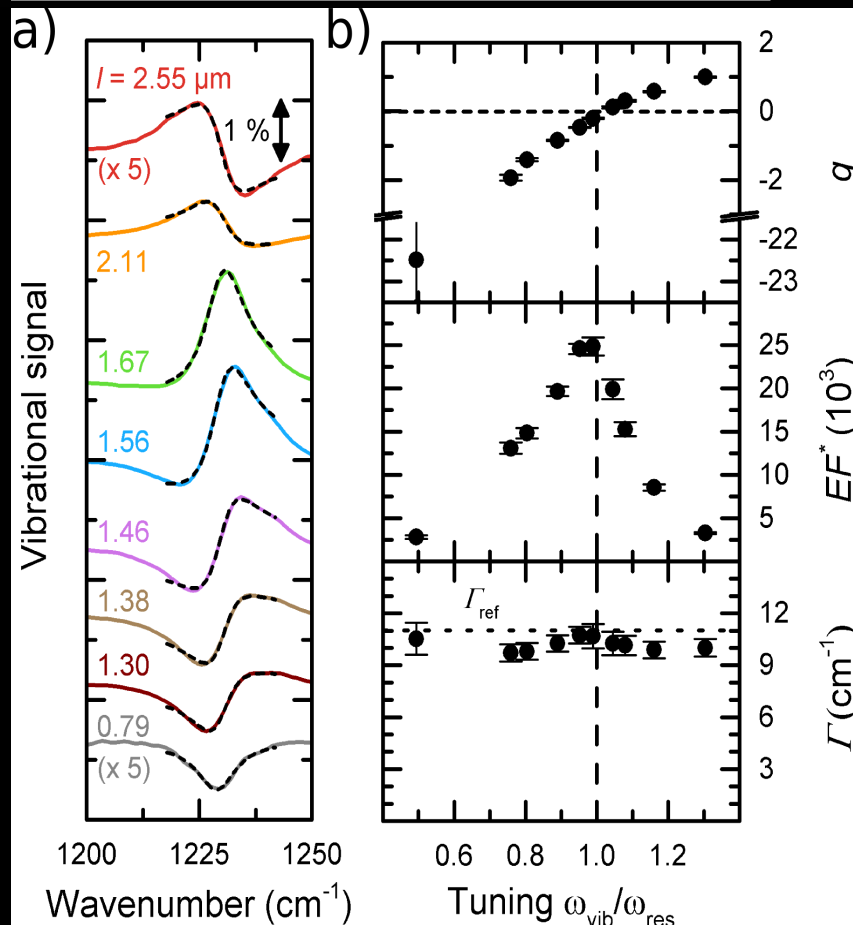

Maximum SEIRA below extinction experimentally established!

J. Vogt et al. Phys. Chem. Chem. Phys. 17 (2015), 21169-21175.

SPATIAL RANGE OF SEIRA

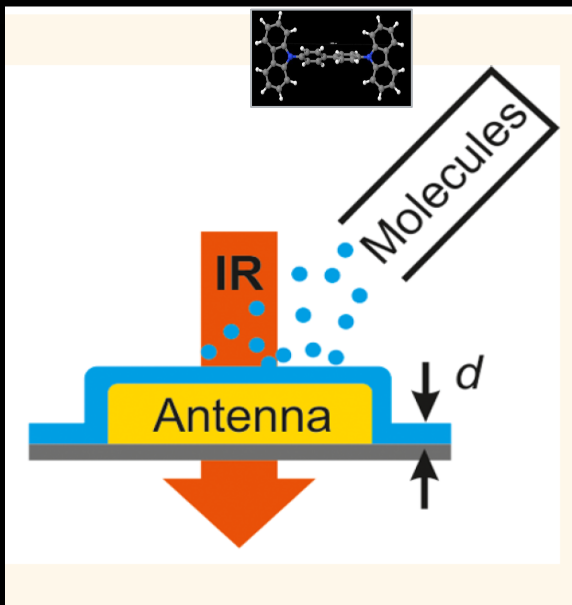

IR spectroscopy during CBP deposition onto a large array (under UHV conditions, 300 K)

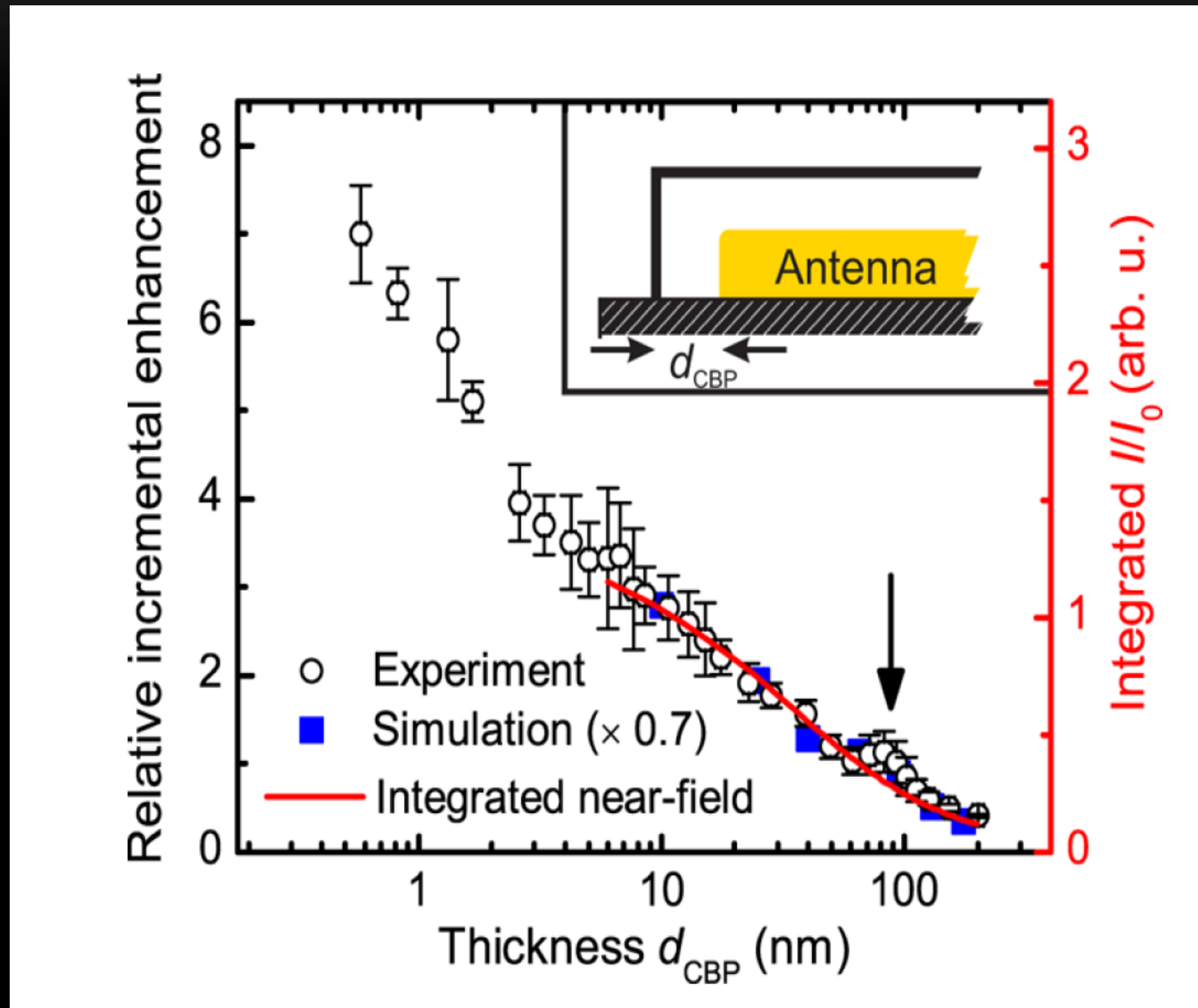

F. Neubrech et al., ACS Nano 8, 6250 (2014)

ROUTES TOWARDS MAXIMUM SEIRA

Reduced substrate polarization and optical cavities

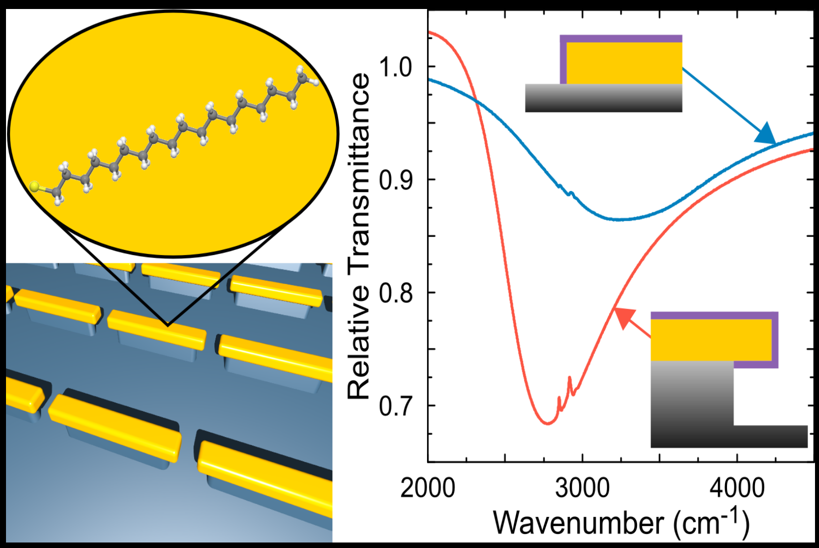

C. Huck, et al., ACS Photonics 2, 4 (2015) 497-505.

Narrow gaps

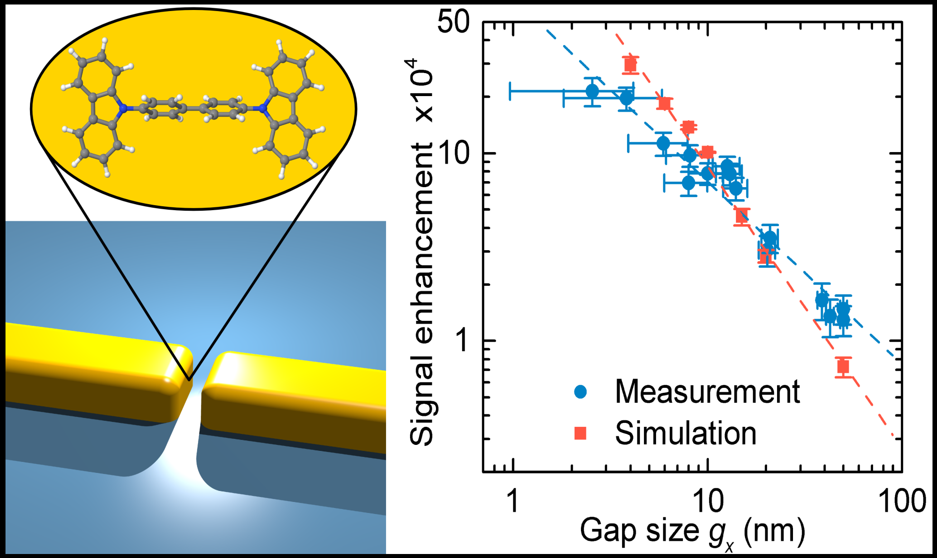

C. Huck, et al., ACS Nano 8, 4908 (2014).

TOWARDS SEIRA OF A SINGLE DUST PARTICLE –APPERTURES FOR BETTER TRAPPING AND HIGHER SEIRA

Nanoslits versus nanorods: Arrays with the same distances, structures with the same width and height and similar length.

SEIRA signals for the slit array are ca. 3 times higher (ODT test molecules).

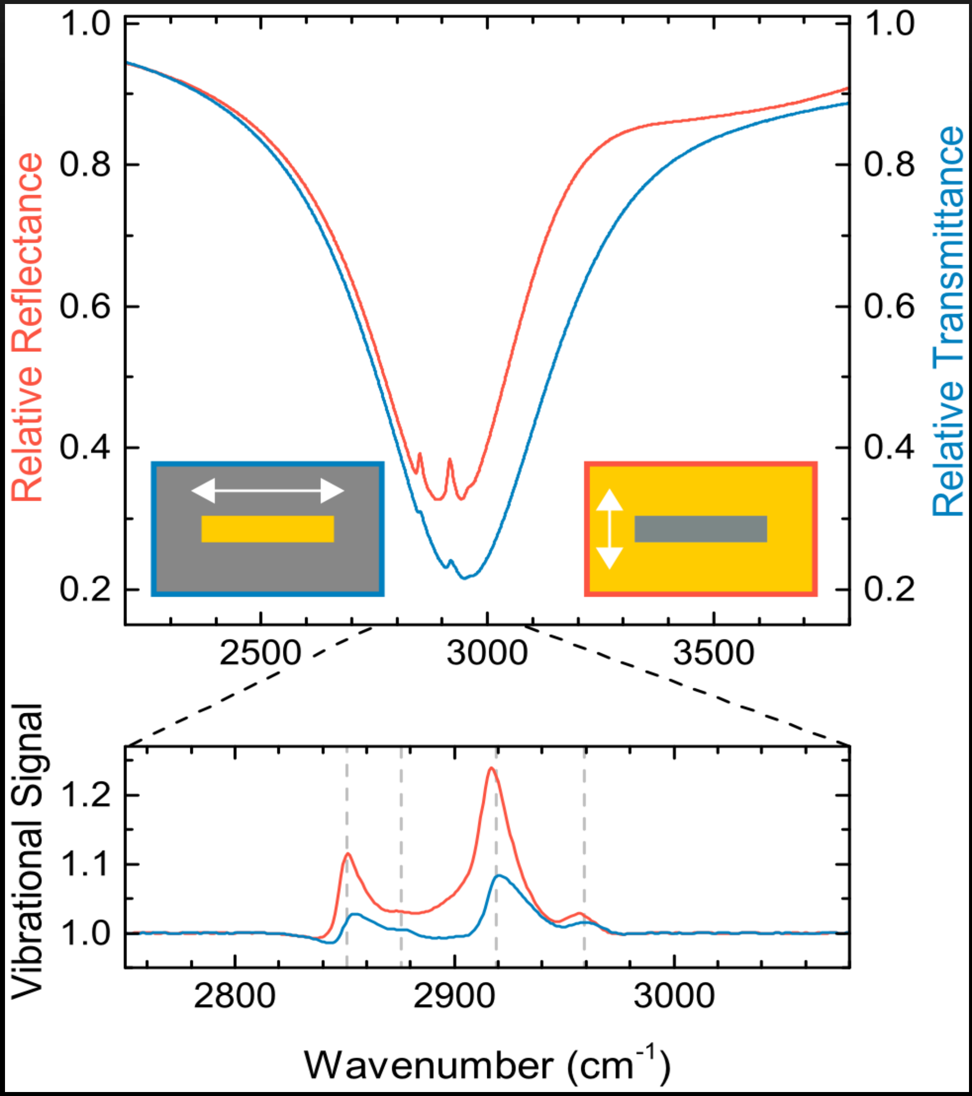

C. Huck et al., ACS Photonics 2, 1489 (2015).

IMPROVED SENSITIVITY AND TRAPPING FOR ULTRAFINE DUST SENSING

C. Huck et al., Phys. Rev. Applied 11, 014036 (2019)

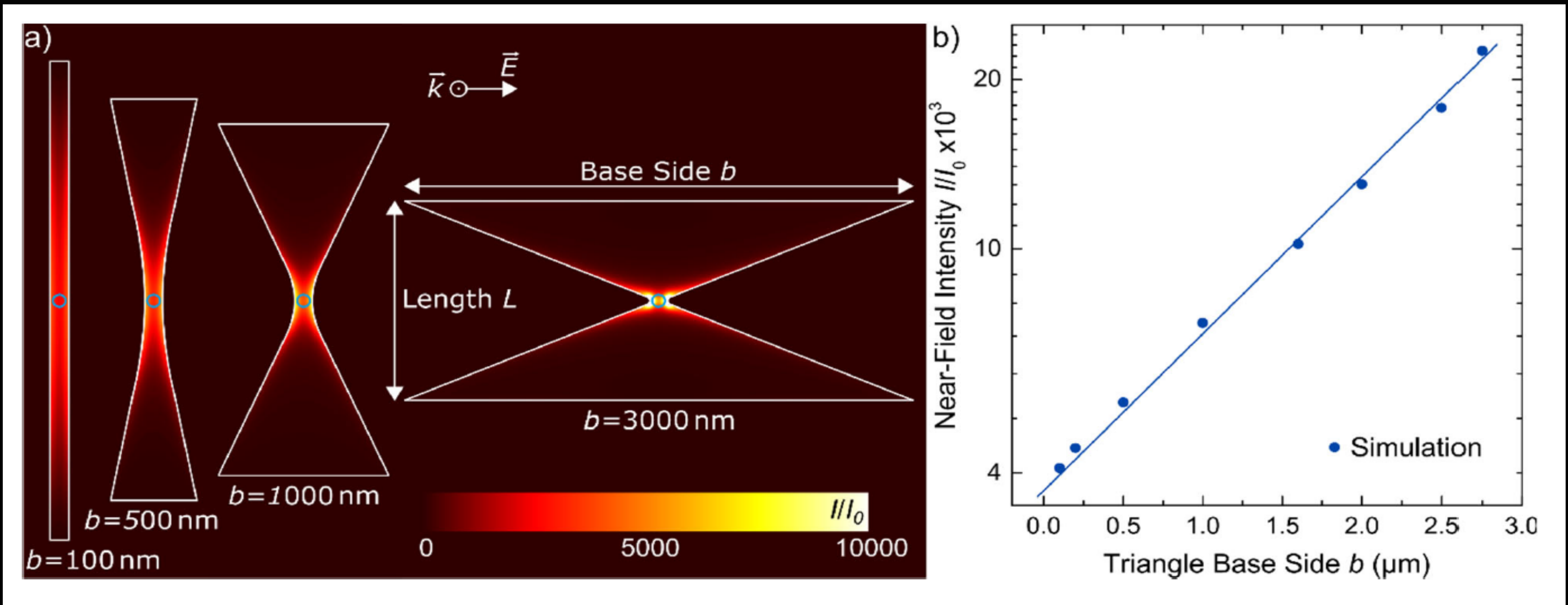

SEIRA SIGNALS OF SILICA NANO-SPHERES

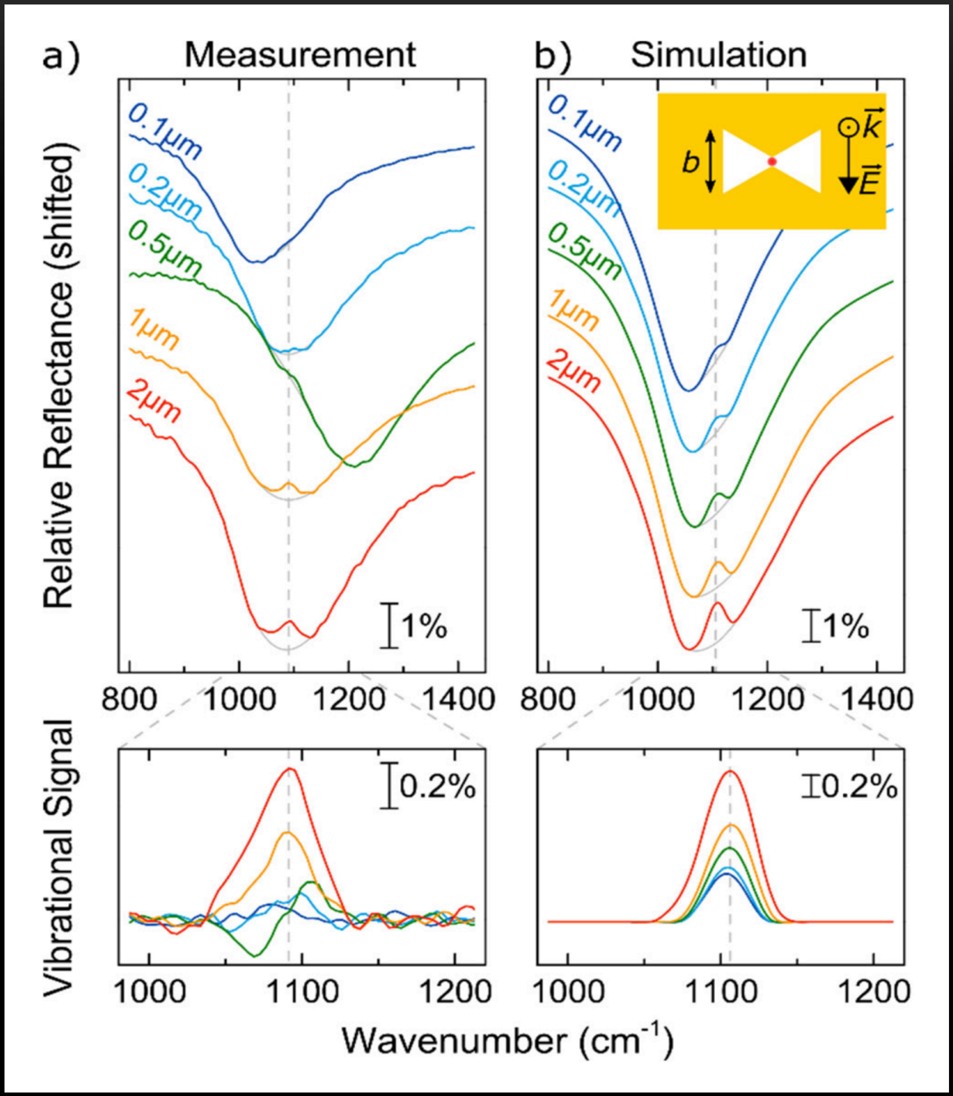

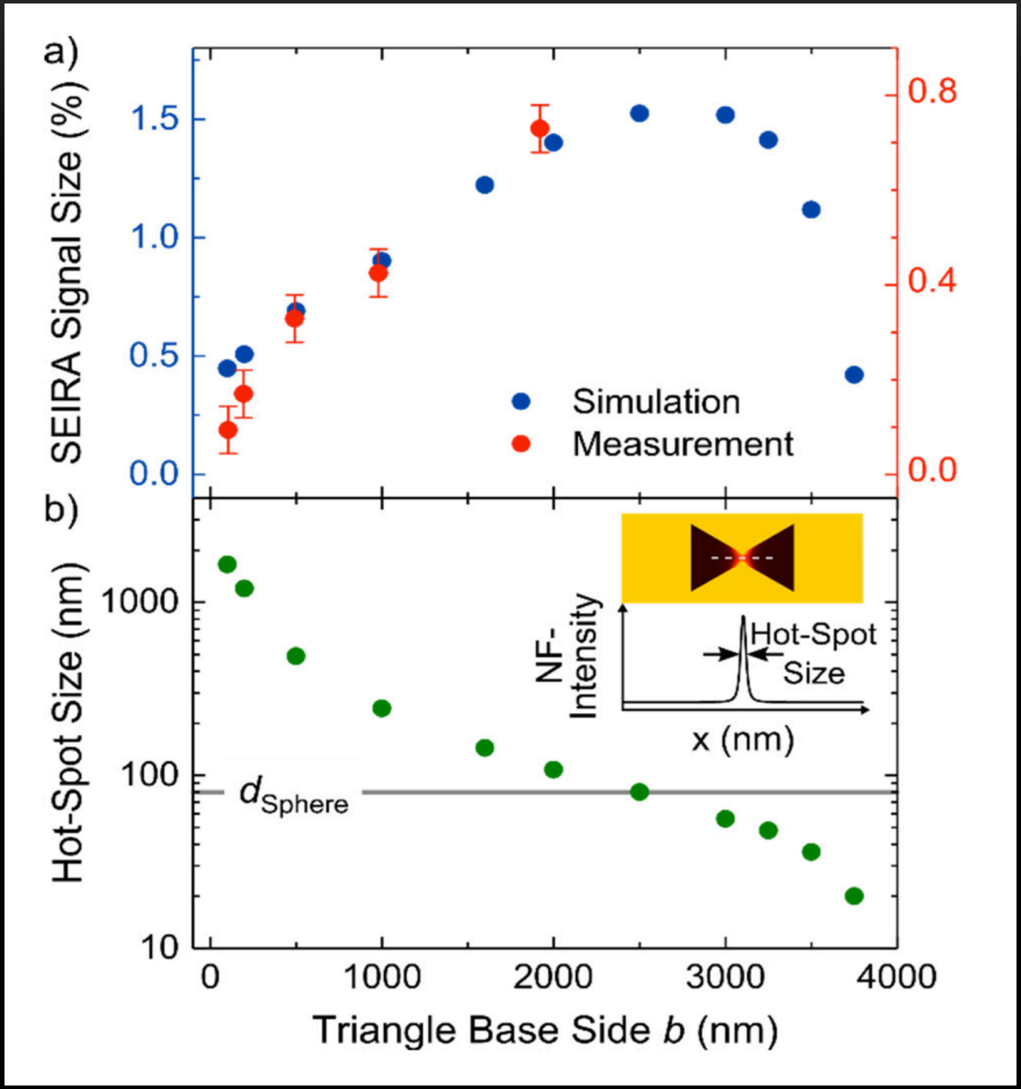

C. Huck et al., Phys. Rev. Applied 11, 014036 (2019)

SENSITIVITY AND DETECTION LIMIT

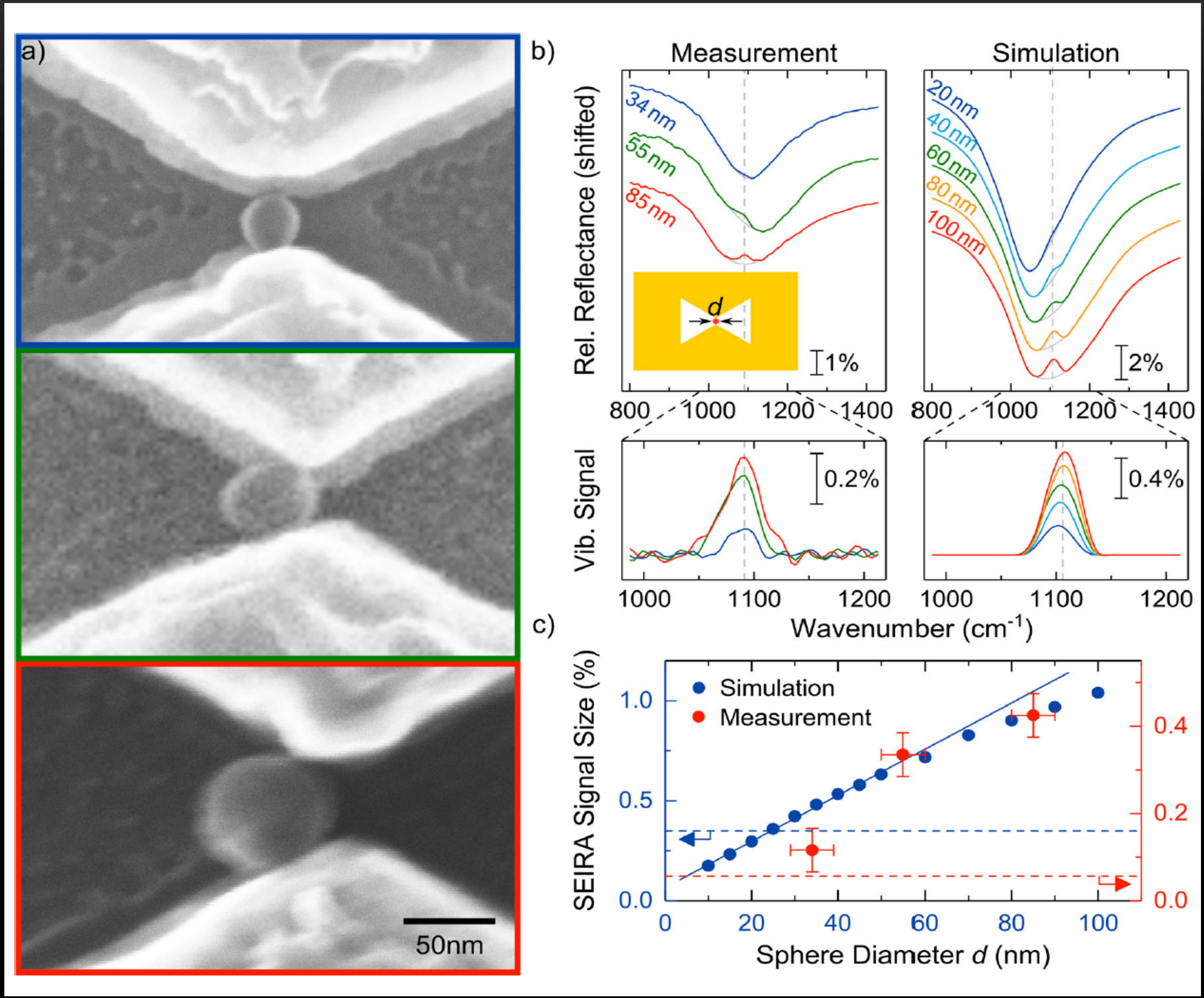

C. Huck et al., Phys. Rev. Applied 11, 014036 (2019)

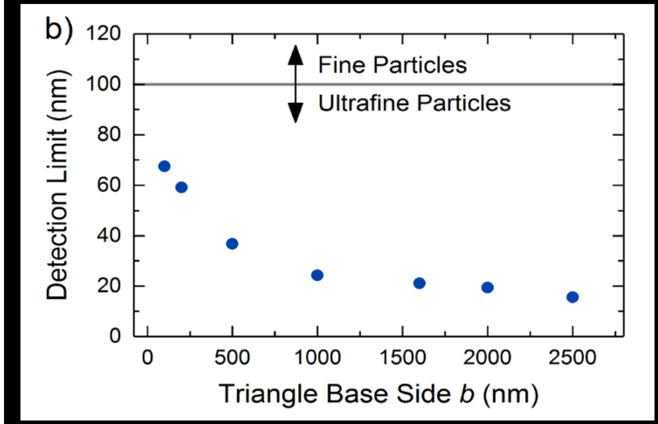

Vicinal Si surfaces as templates for atomic chains

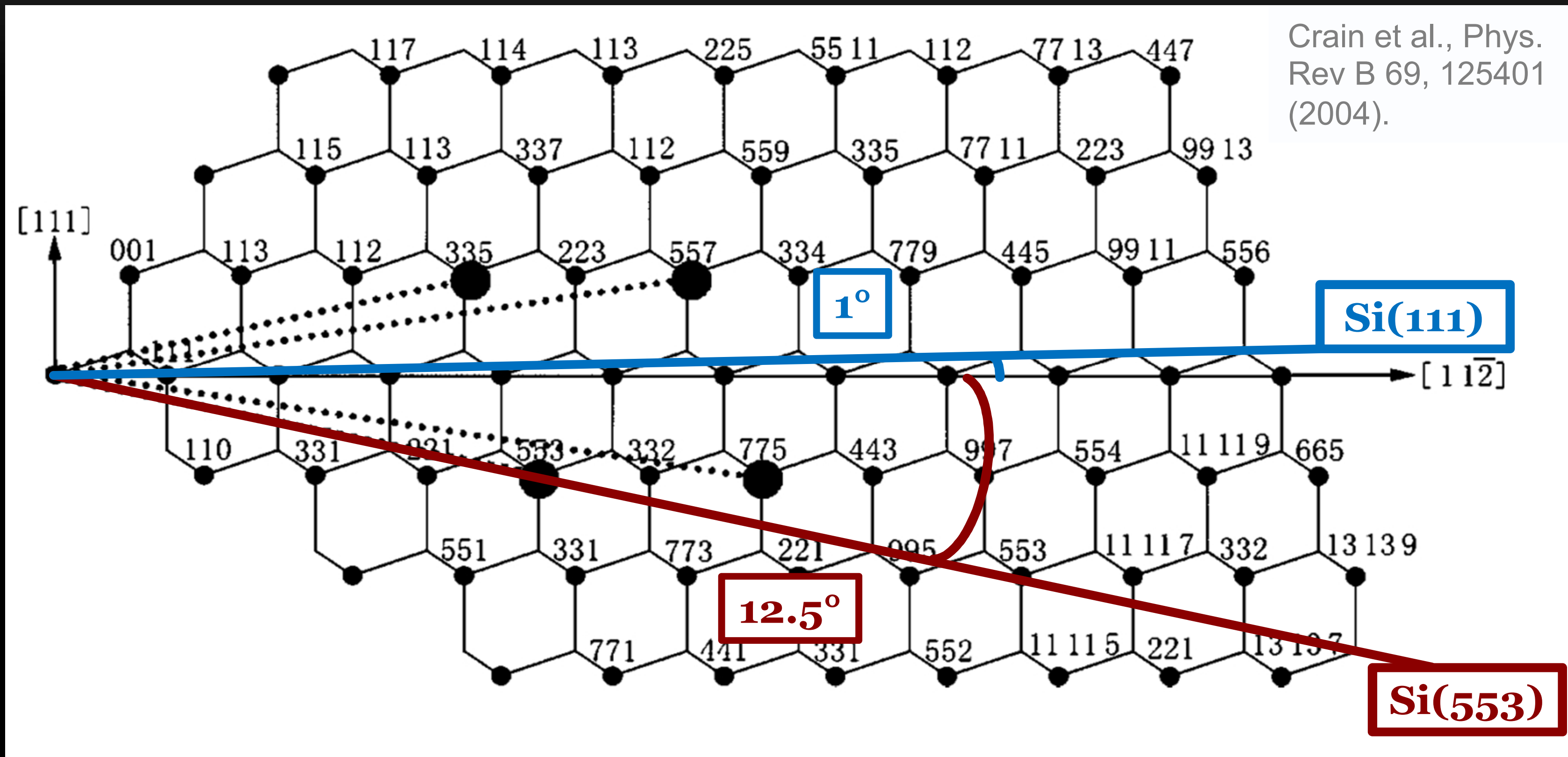

Vicinal Si surfaces as templates, examples

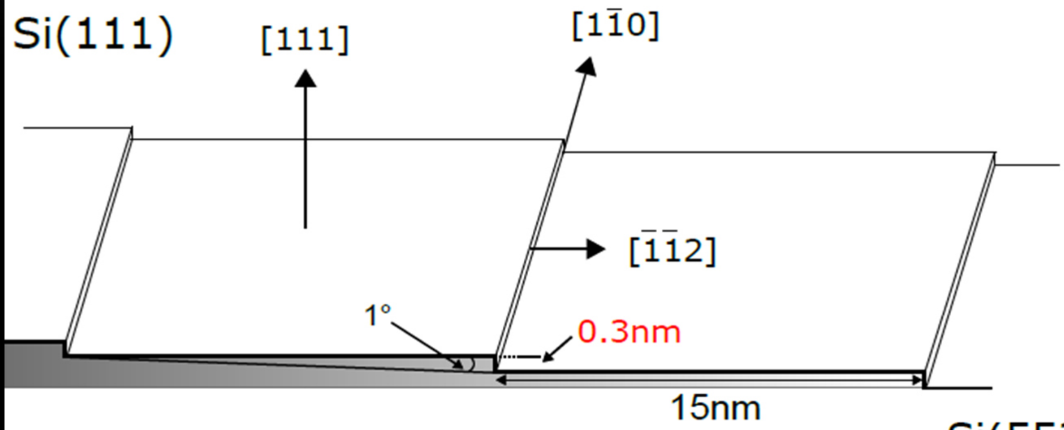

	Si(111)	Si(553)
angle	1° in $[\bar{1}\bar{1}2]$	12.5° in $[11\bar{2}]$
step height	0.26 nm	0.33 nm
step width	15 nm	1.48 nm

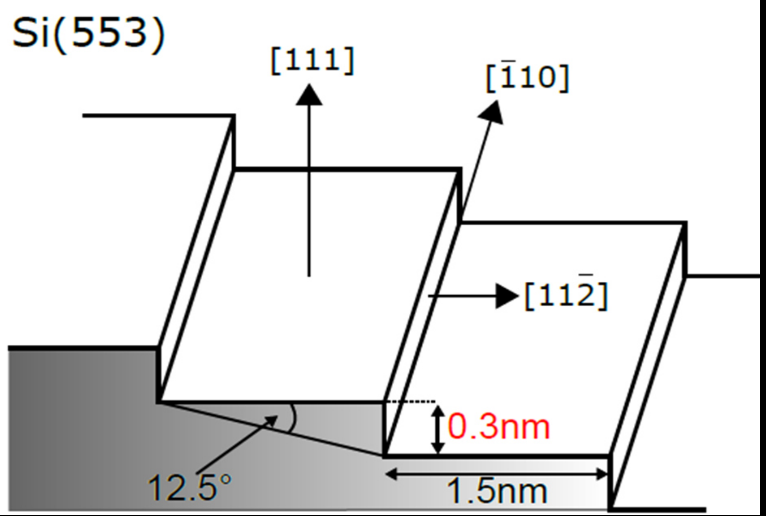

N. Galden, bachelor thesis, Univ. Heidelberg 2015

Vicinal Si surfaces with Au

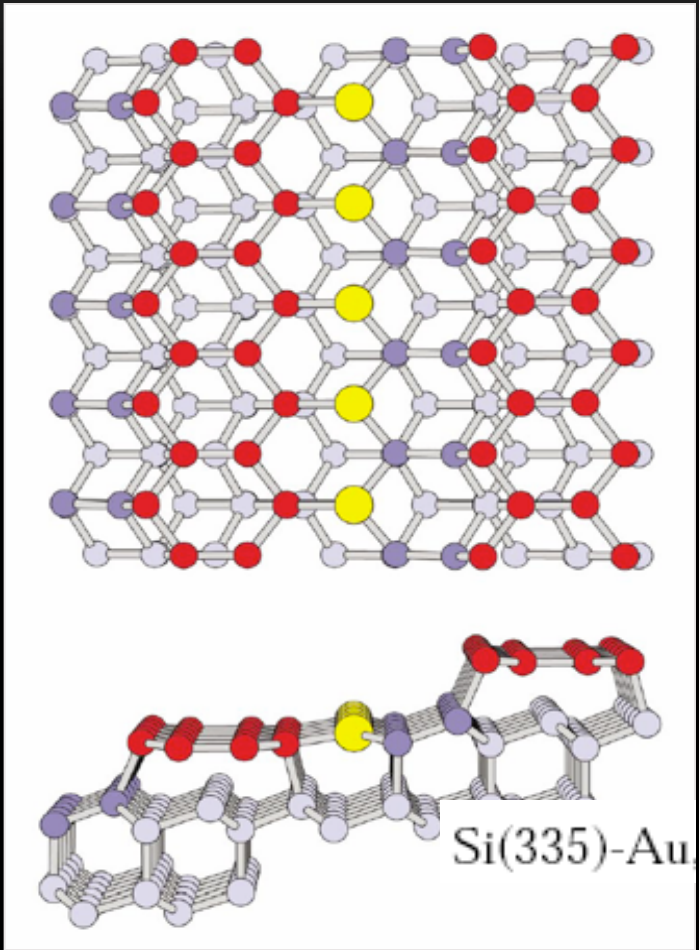

PHYSICAL REVIEW B **69**, 125401 (2004)

TABLE I. Summary of chain spacings, gold coverages, and tilt angles from [1 1 1] for several gold chain structures on vicinal silicon surfaces. The coverages are in units of Si(111) monolayers (ML).

Orientation	Spacing (nm)	Au coverage (ML)	Off-axis angle
Si(111) 5×2-Au	1.67	0.4 (new: 0.7)	0°
Si(335)-Au	1.26	0.27±0.04	14.4° to $[\bar{1}\,\bar{1}\,2]$
Si(557)-Au	1.92	0.18±0.04	9.5° to $[\bar{1}\,\bar{1}\,2]$
Si(553)-Au	1.48	(HCW:0.46)	12.5° to $[1\,1\,\bar{2}]$
Si(775)-Au	2.13	0.25±0.07	8.5° to $[1\,1\,\bar{2}]$
Si(995)-Au	2.63	0.13±0.04	13.8° to $[1\,1\,\bar{2}]$
Si(13 13 7)-Au	3.78	0.09±0.04	14.4° to $[1\,1\,\bar{2}]$
Si(110) 5×2-Au	2.72	0.30±0.07	35.3° to $[1\,1\,\bar{2}]$

Examples by STM

Indium on Si(111)

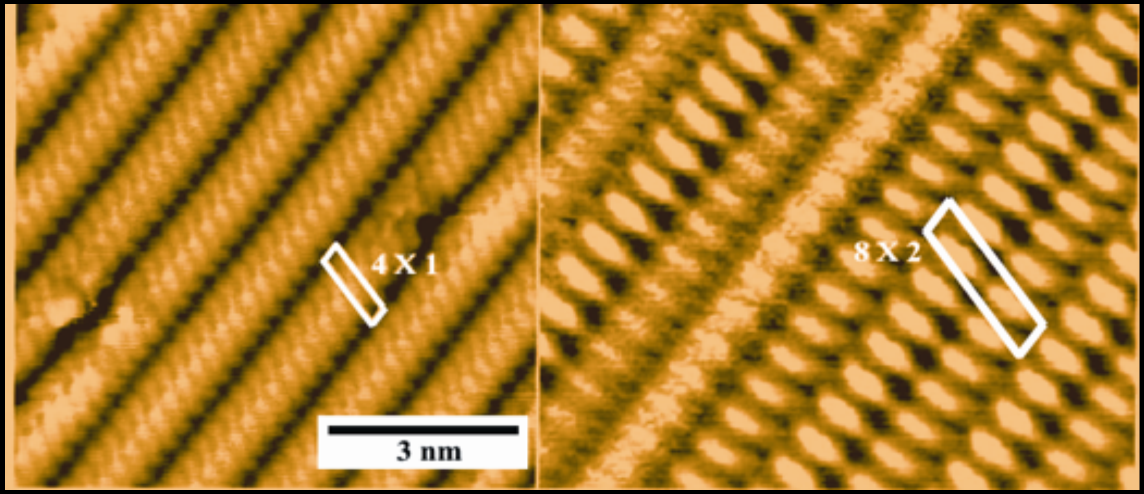

H.W. Yeom et al, Phys. Rev. Lett. **82**, 4898 (1999)

Gold on Ge(001)

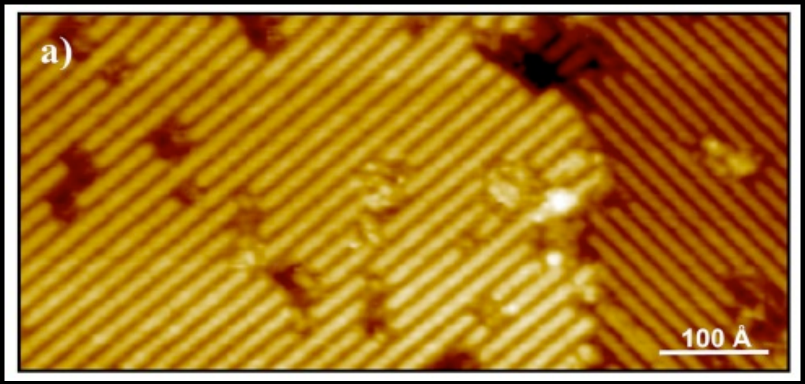

J. Schaefer et al, Phys. Rev. Lett. **101**, 236802 (2008)

In reality, there are domains and thus finite lengths of the metal-atom chains.

Localized quasi-1D IR plasmonic excitations

$$\omega_{\text{res}}(L) = \frac{e\pi}{L}\left\{\frac{1}{2\varepsilon_0\varepsilon_{\text{effective}}}\cdot\frac{n_{\text{1D}}}{m^*}\ln\left(\frac{L}{\pi b}\right)\right\}^{\frac{1}{2}}$$

For plasmonic dispersion relations see, *e.g.*, T. Giamarchi, Quantum Physics in One Dimension", Clarendon Press, Oxford 2003. Here *π/L* is inserted as wavevector of the standing wave.

b is a measure of the spill-out of the electronic wavefunction. n_{1D} is the 1D free charge carrier density, m^* their effective mass.

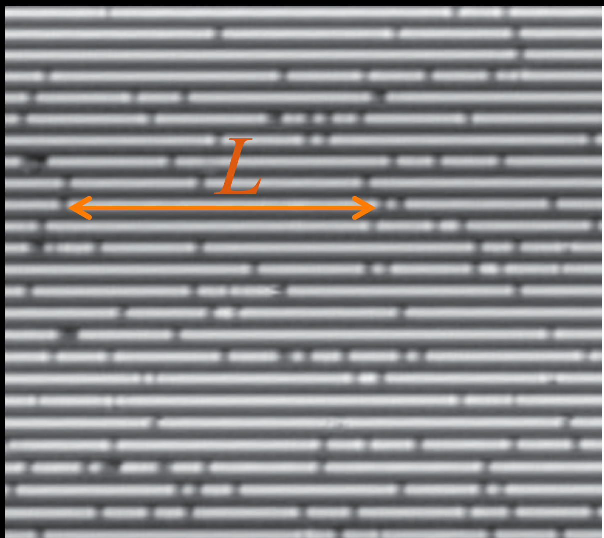

STM image (ca. 38 nm x 38 nm) of **finite chains** of a Si(553)-Au surface. J.N. Crain et al., Phys. Rev. Lett. 96 (2006) 156801.

- The fundamental antenna-like mode for $L=\lambda_{\text{plasmon}}/2$ has a dipolar character and interacts with light
- Absorption cross section of dipolar plasmonic excitations of metallic needles:

$$\sigma_{\text{abs}} = \frac{n_{1D}Le^2}{m^*\varepsilon_0 c}\frac{\omega^2\omega_\tau}{\left[\left(\omega_{\text{res}}^2-\omega^2\right)^2+\omega^2\left(\omega_\tau\right)^2\right]}$$

F. Hötzel et al., Nano Lett. 15, 4155 (2015); J. Phys. Chem Lett. 6, 3615 (2015); J. Phys. Chem. C 121, 8120 (2017).

Si (111)-(4x1) In, plasmonic resonances of finite In atom chains, two different domain sizes

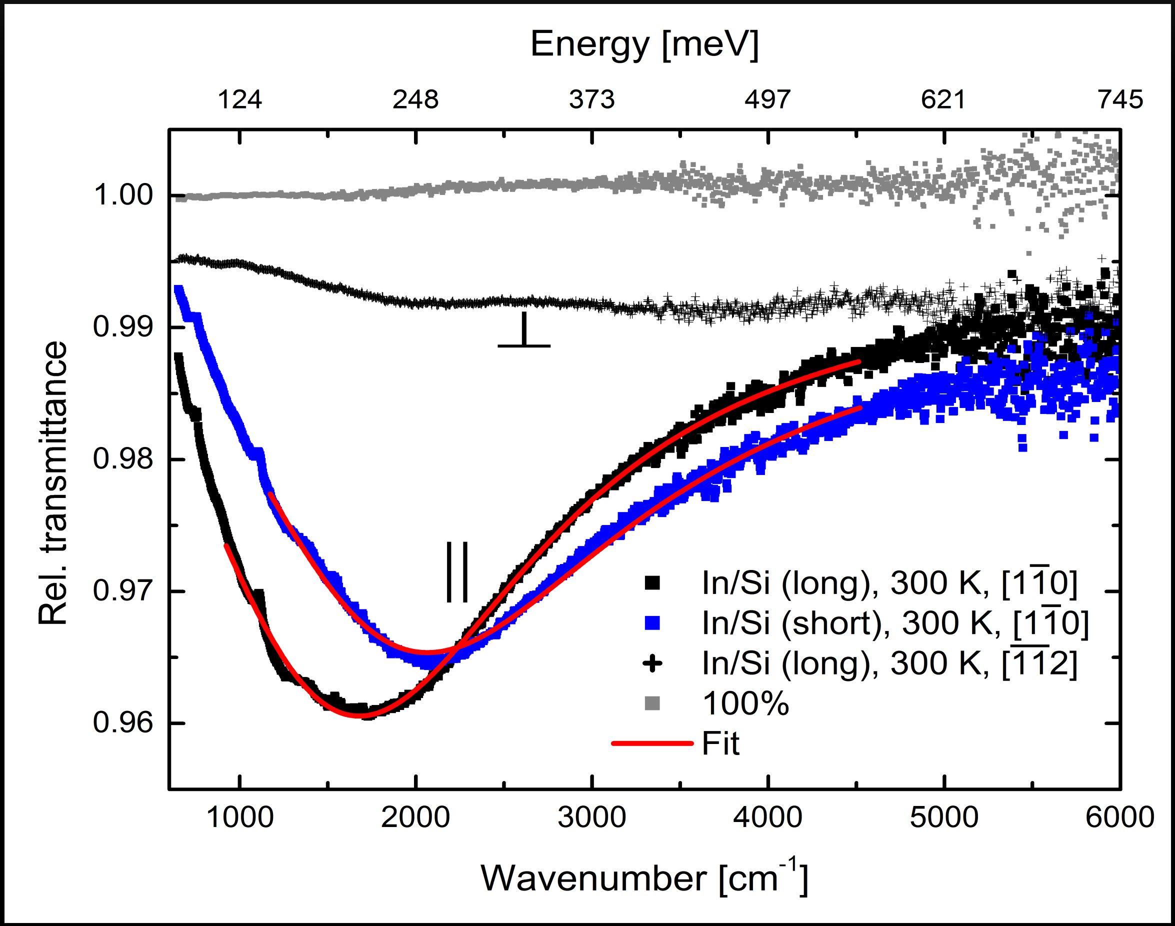

H. V. Chung et al., Applied Physics Letters 96 (2010) 243101.
F. Hötzel et al., Nano Letters 2015, SI

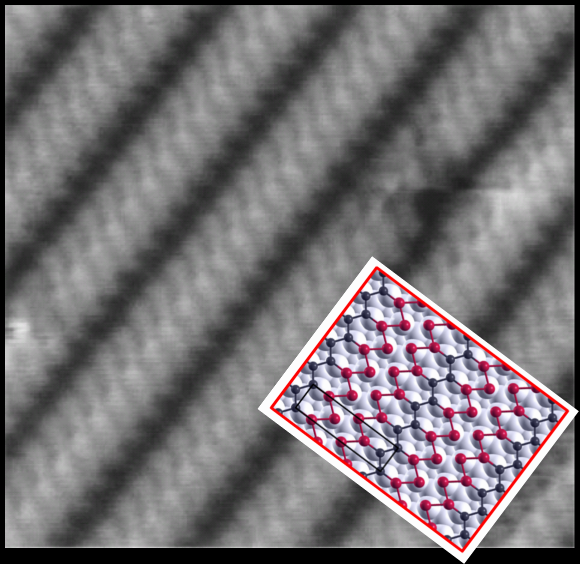

STM, Si(111)-4x1-In (room temperature), from T. Nagao 2010, model e.g. by W.G. Schmidt et al. 2012, red: In.

The Si (111)-(5x2) Au surface

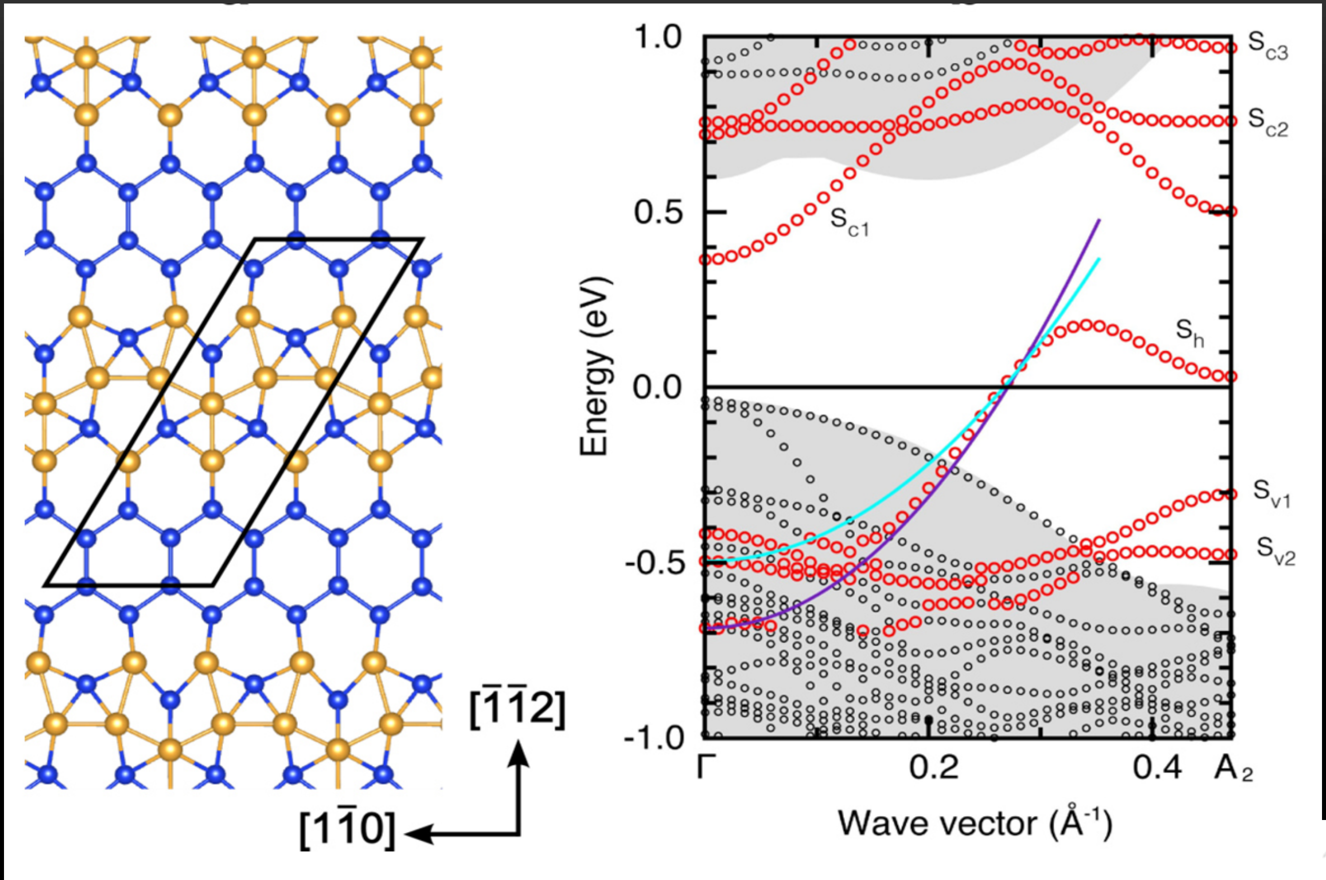

DFT calculated band structure (Seino, Bechstedt), two possible parabolic fits of the half-filled band S_h are indicated in purple and turquois.

F. Hötzel, et al., Nano Letters 15, 4155 (2015).

RHEED, 20 K,
Si wafer with a slight miscut (1°) towards [-1 -1 2] supports the formation of one dominating domain orientation.

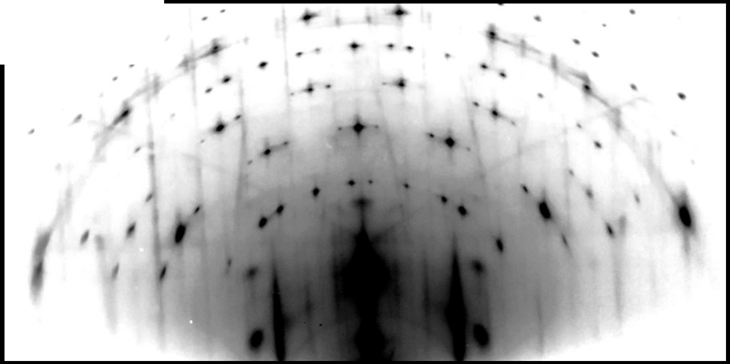

Au on Si (111)-(5x2) Au
Plasmonic resonances disappear upon S_h band filling

Au deposition at 300 K,

A reconstruction change could not be seen.

DFT calculations by K Seino and F. Bechstedt demonstrate that with 0.8 ML (8 Au in unit cell) the S_h band has shifted below the Fermi level.

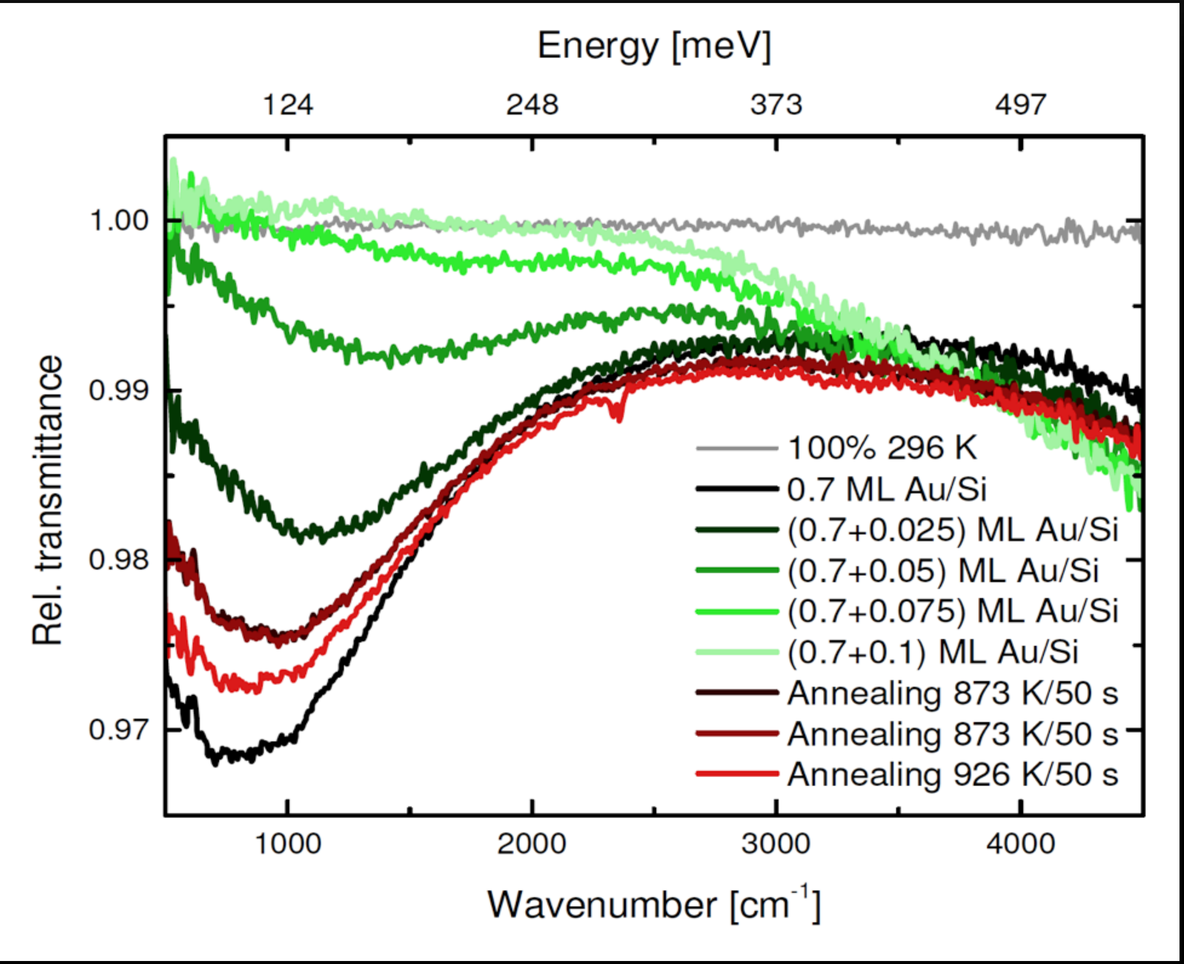

F. Hötzel, et al., J. Phys. Chem Lett. 6, 3615 (2015).

GOLD-ATOM CHAINS ON SI(553) – HIGH COVERAGE

0.46 ML Au

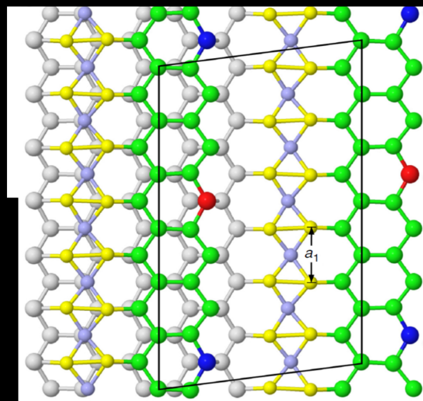

S.C. Erwin and F.J.Himpsel, Nat. Commun.1 (2010) 58.

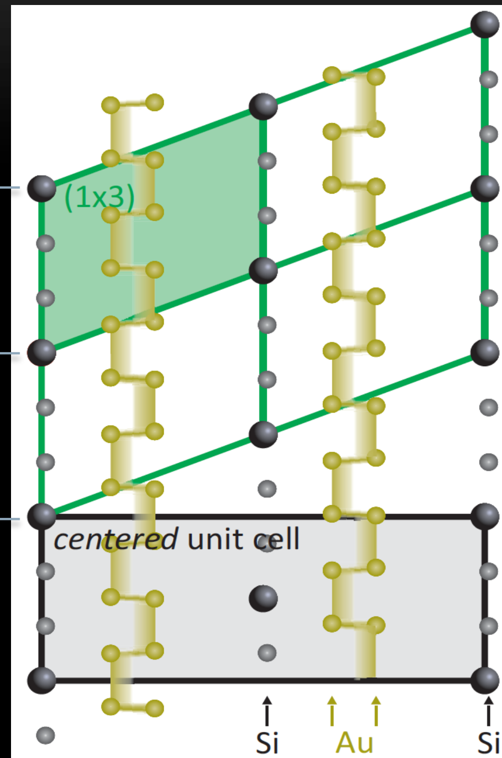

B. Hafke et al., Phys. Rev. B 94 (2016) 161403.

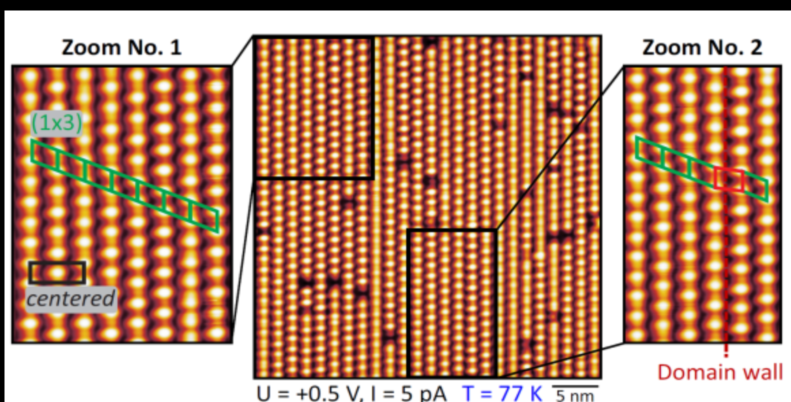

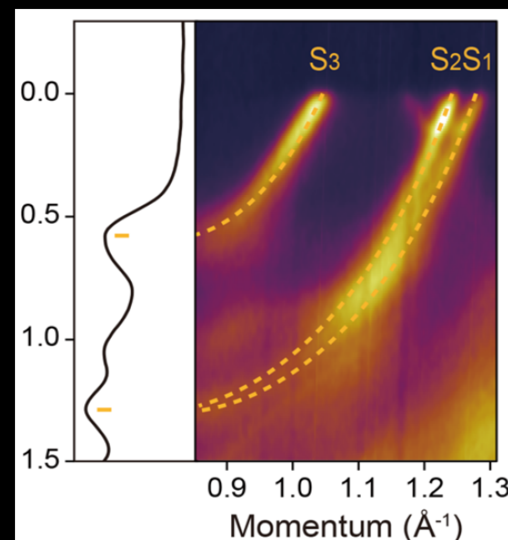

I. Song et al., ACS Nano 9 (2015) 10621.

PLASMON DISPERSION OF AU CHAINS ON SI(553)

Dispersion from EELS, far below the light line

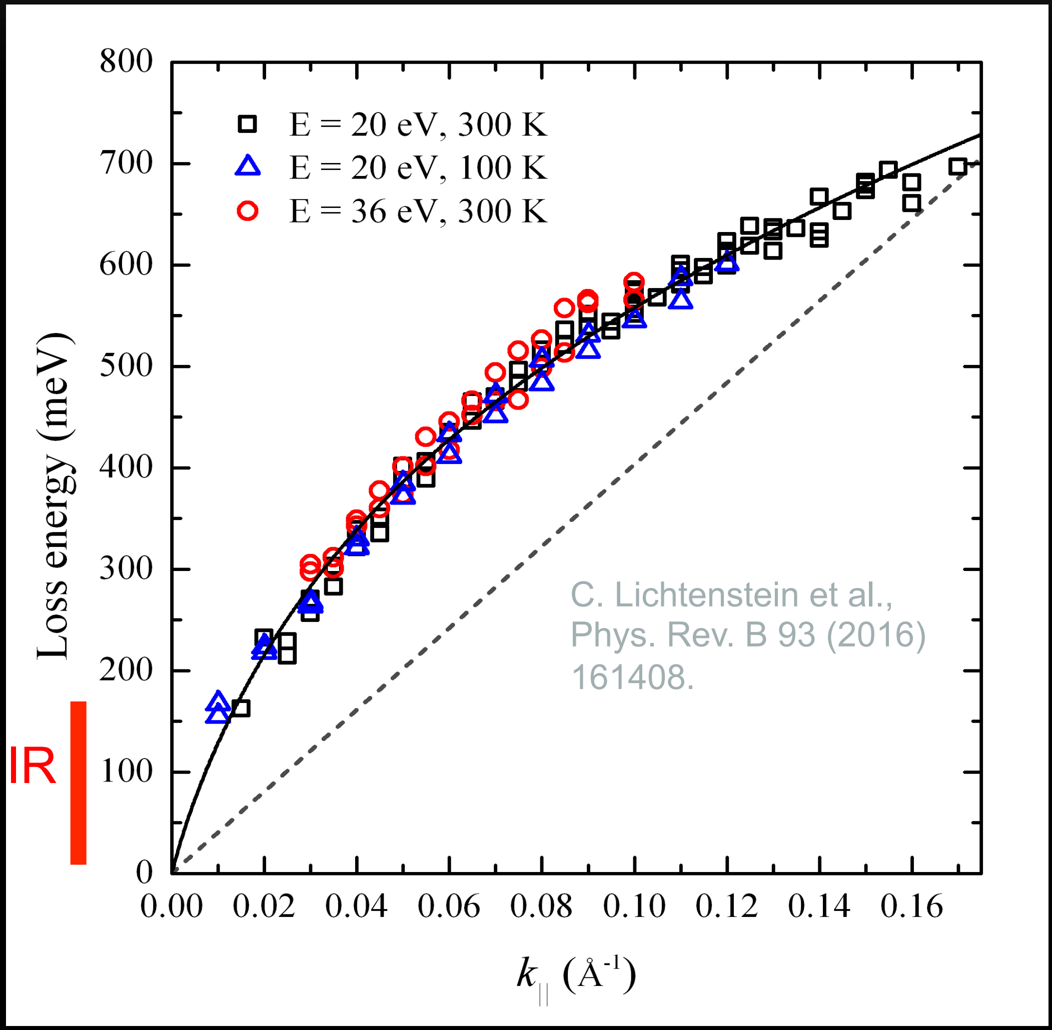

Adsorbate molecules on Au chains on Si(553)

The primitive unit cell in comparison to the adsorbate molecules

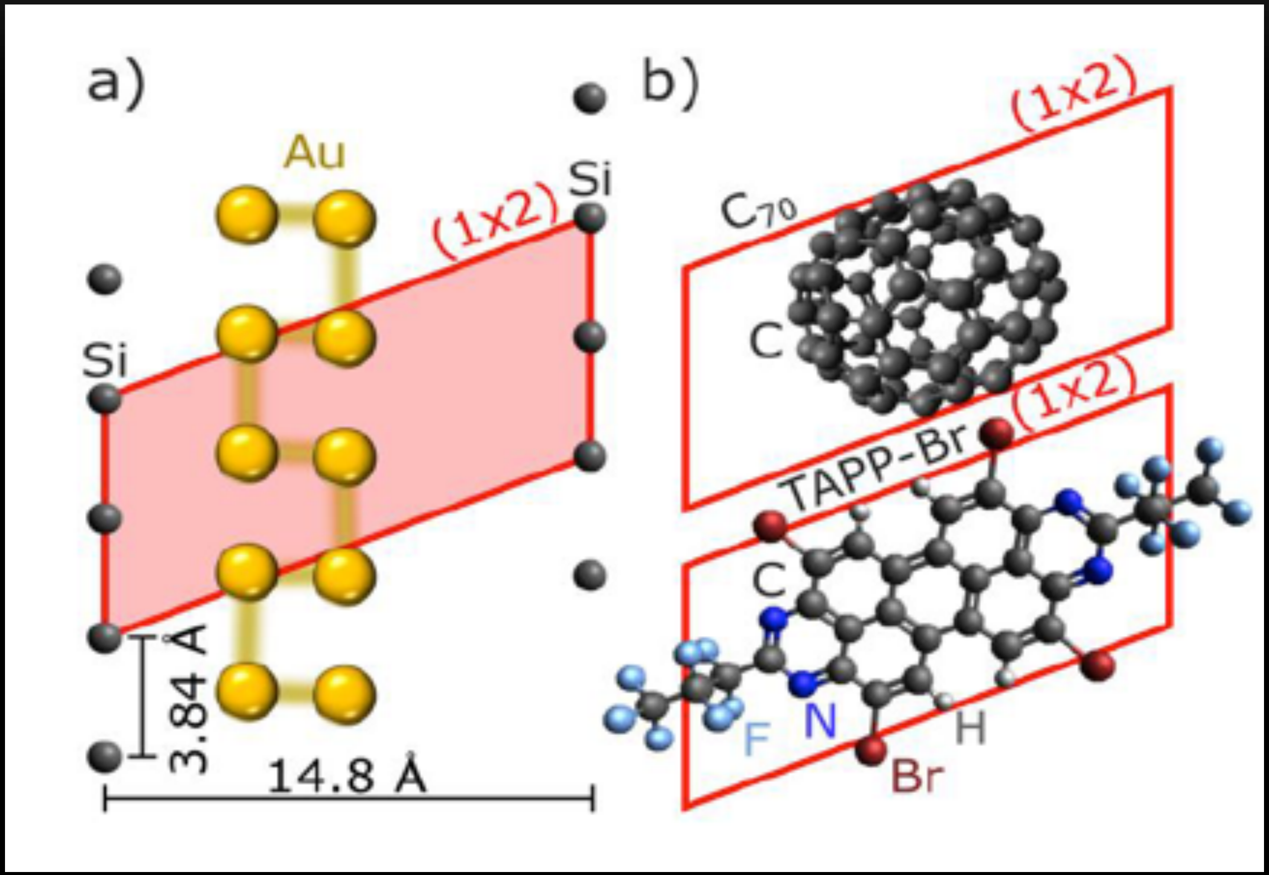

B. Hafke et al., Phys.Rev.B 94, 161403(R) (2016).

1 ML ca.
1 molecule per unit cell

TAPP-Br (2,9 Bis (heptafluoropropyl) 4,7,11,14 tetrabromo 1,3,8,10 tetraazaperopyrene) is a N-heteropolycycle,
see Geib et al., Adv. Funct. Mater. 2013, 23, 3866.
The molecules seem to be promising for the usage as organic n-channel semiconducting materials (as C_{70}).

M. Tzschoppe et al., Surface Science 2018, doi.org/10.1016/j.susc.2018.02.007;
M. Tzschoppe et al., J.Physics: Condensed Matter, 31 (2019) 195001.

C_{70} ON AU CHAINS ON SI(553), IR SPECTRA

AT 300 K

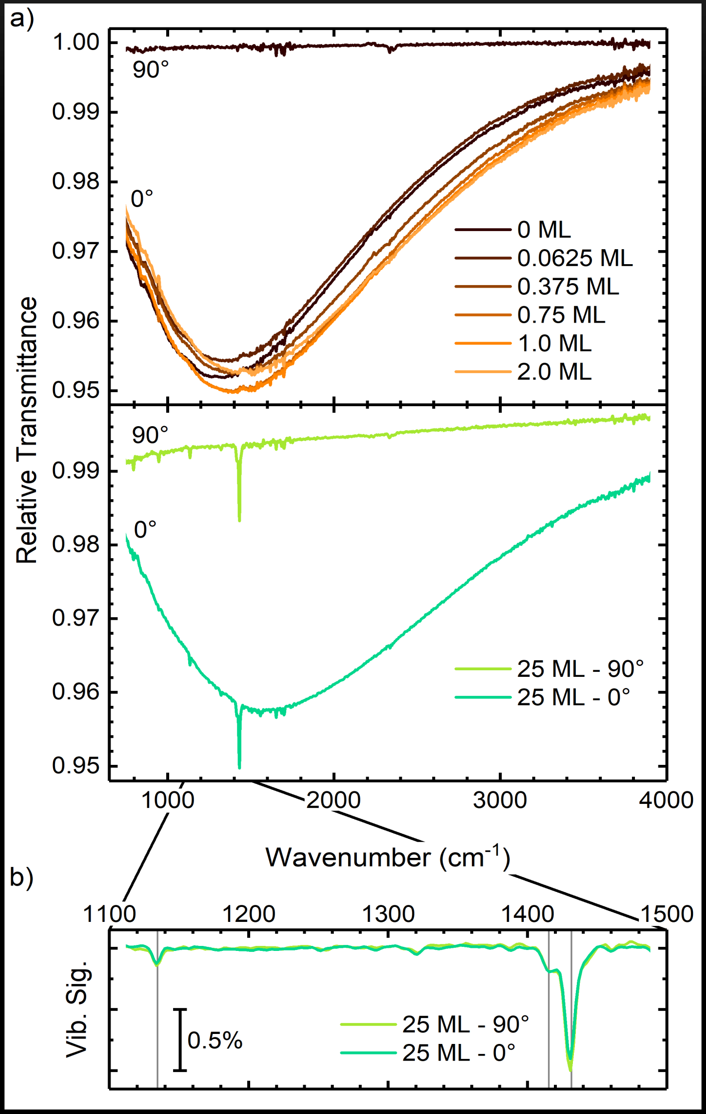

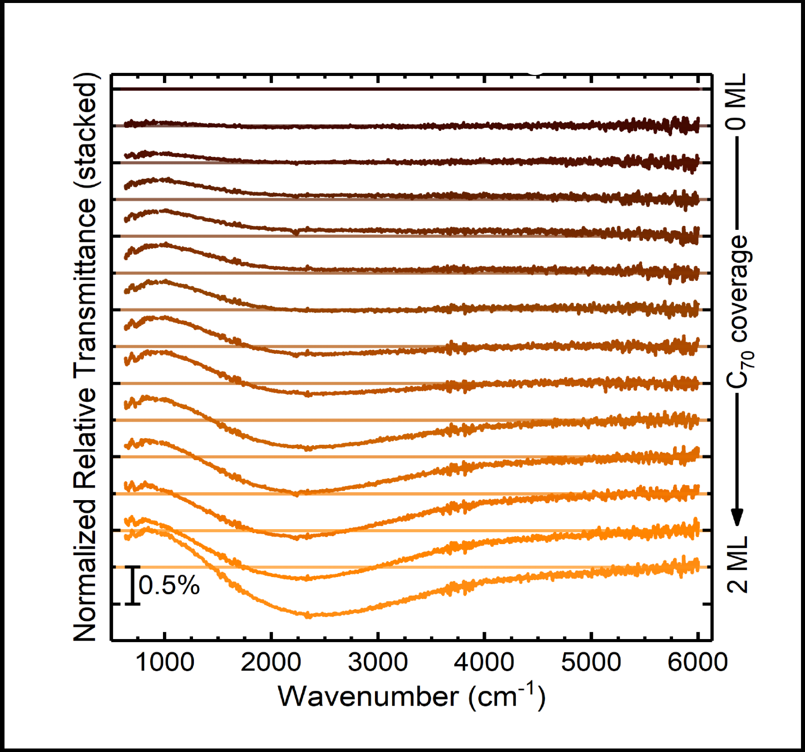

M. Tzschoppe et al., Surface Science 2018, doi.org/10.1016/j.susc.2018.02.007

TAPP-Br on Si(553)-Au, IR spectra, 300 K

Spectra for various TAPP-Br coverage

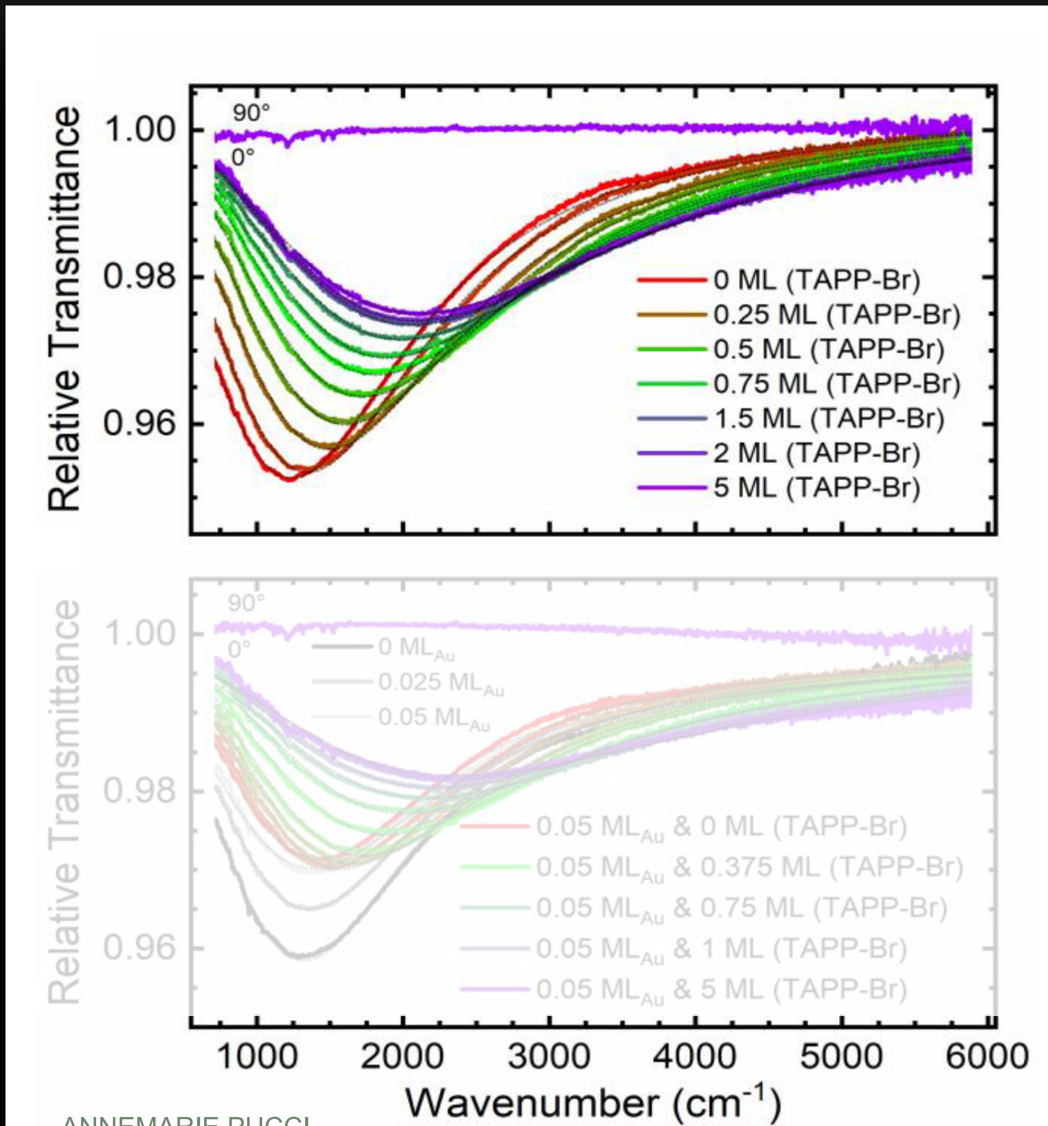

Zoom to vibrational lines*, background corrected spectra

*L. Hahn et al., Chem. Eur. J. 2015, 21, 17691.

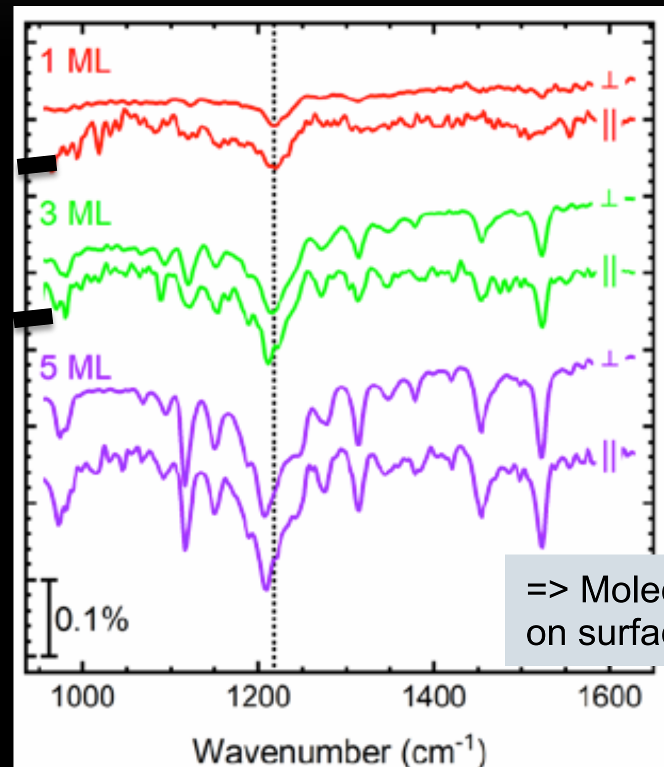

=> Molecules flat on surface

M. Tzschoppe et al., J.Physics: Condensed Matter, 31 (2019) 195001

TAPP-Br on Si(553)-Au, IR spectra, 300 K

Spectra for various TAPP-Br coverage

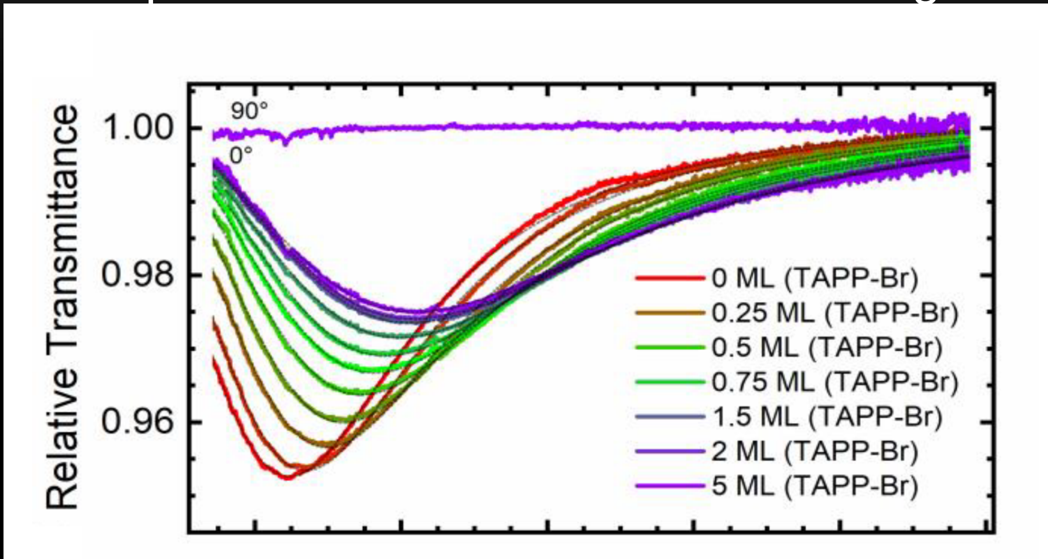

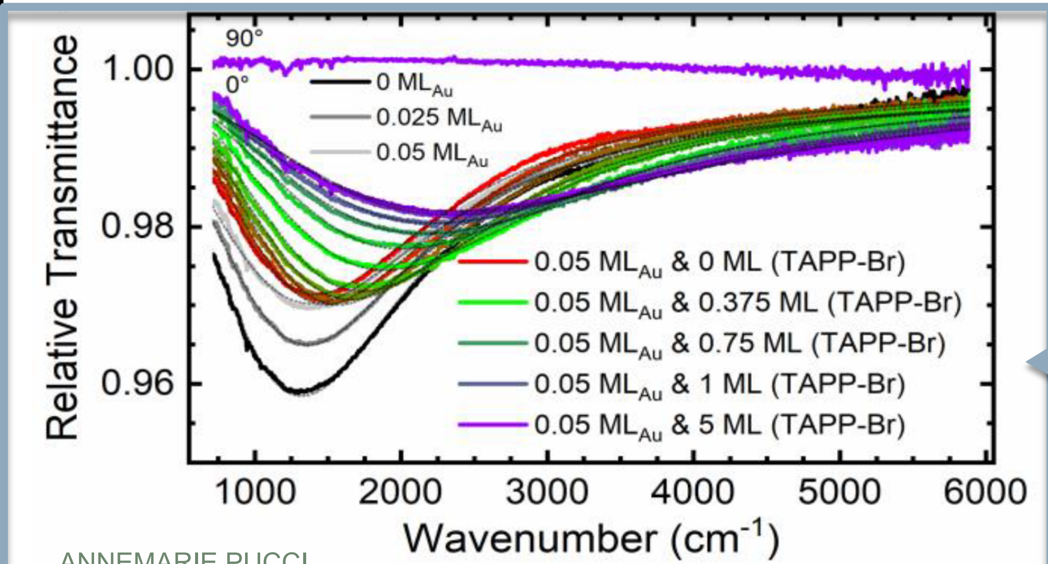

Zoom to vibrational lines*, background corrected spectra

*L. Hahn et al., Chem. Eur. J. 2015, 21, 17691.

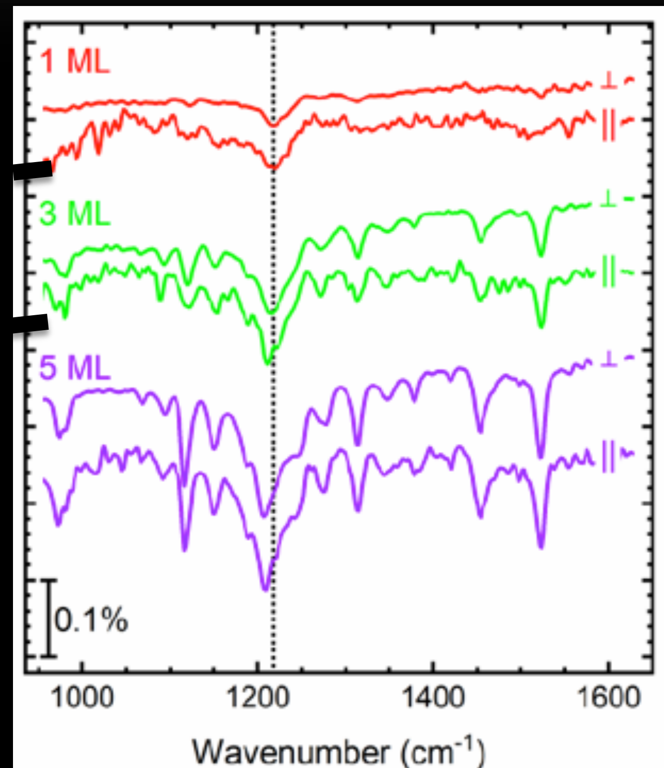

with 0.05 ML Au pre-coverage (electron doping,

Fit results

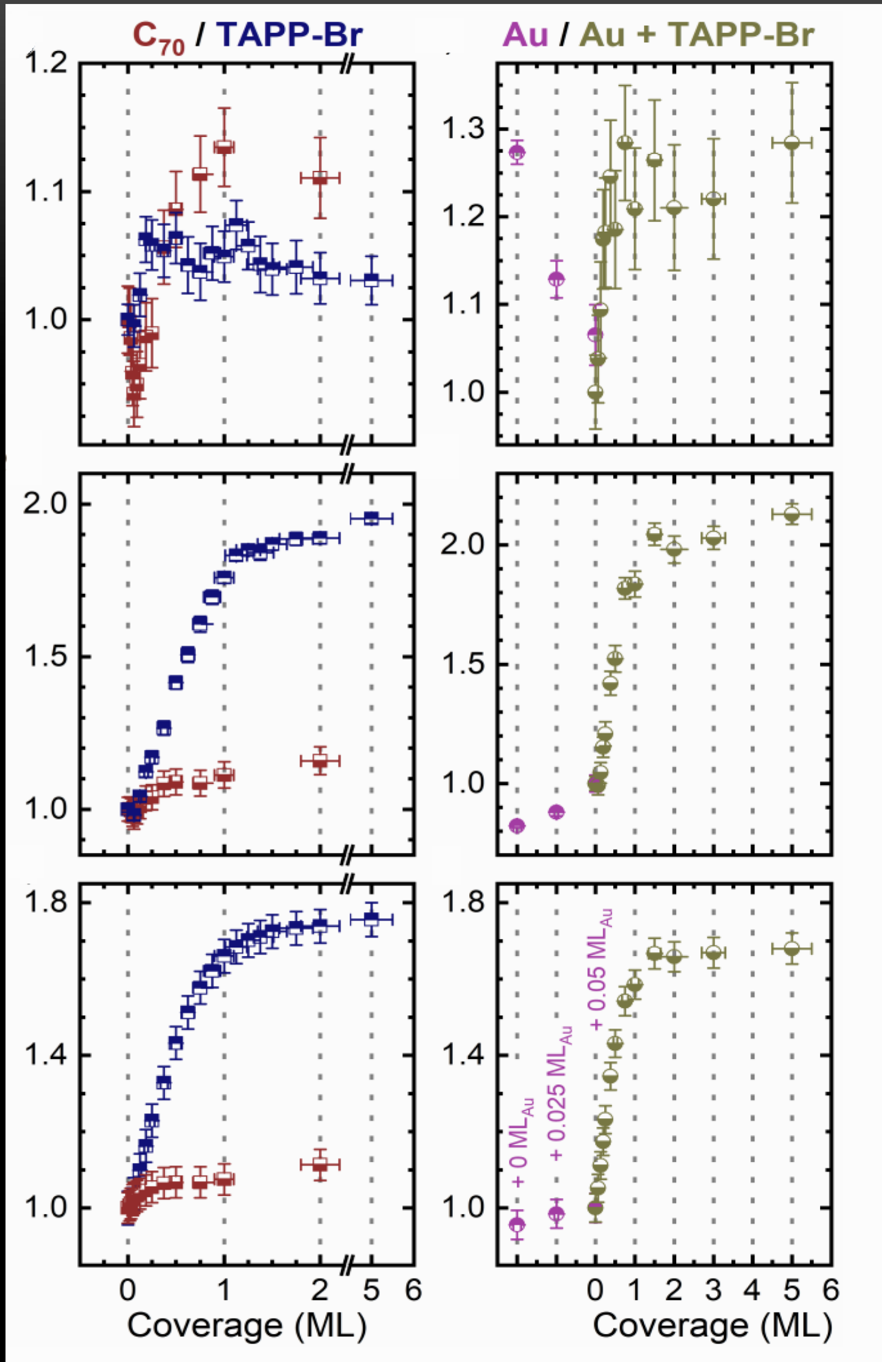

M. Tzschoppe et al., J.Physics: Condensed Matter, 31 (2019) 195001

← relative change of $\frac{n_{1D}}{m^*}$

=> Weak conductivity increase for C_{70} (due to electron extraction), negligible CT for TAPP-Br

← relative change of ω_τ

=> typical „surface friction" effect for C_{70} , extreme increase of electronic damping with TAPP-Br, not seen with TAPP-H

rel. change of

←

$$\omega_{res}(L) \propto \sqrt{\frac{1}{\varepsilon_{effective}} \cdot ln\left(\frac{L}{\pi b}\right)}$$

=> Small increase for C_{70} due to increase in n_{1D}/m^*, TAPP-Br: Decrease of b <=> push back effect (lowers work function)

The pillow (cushion, push back) effect

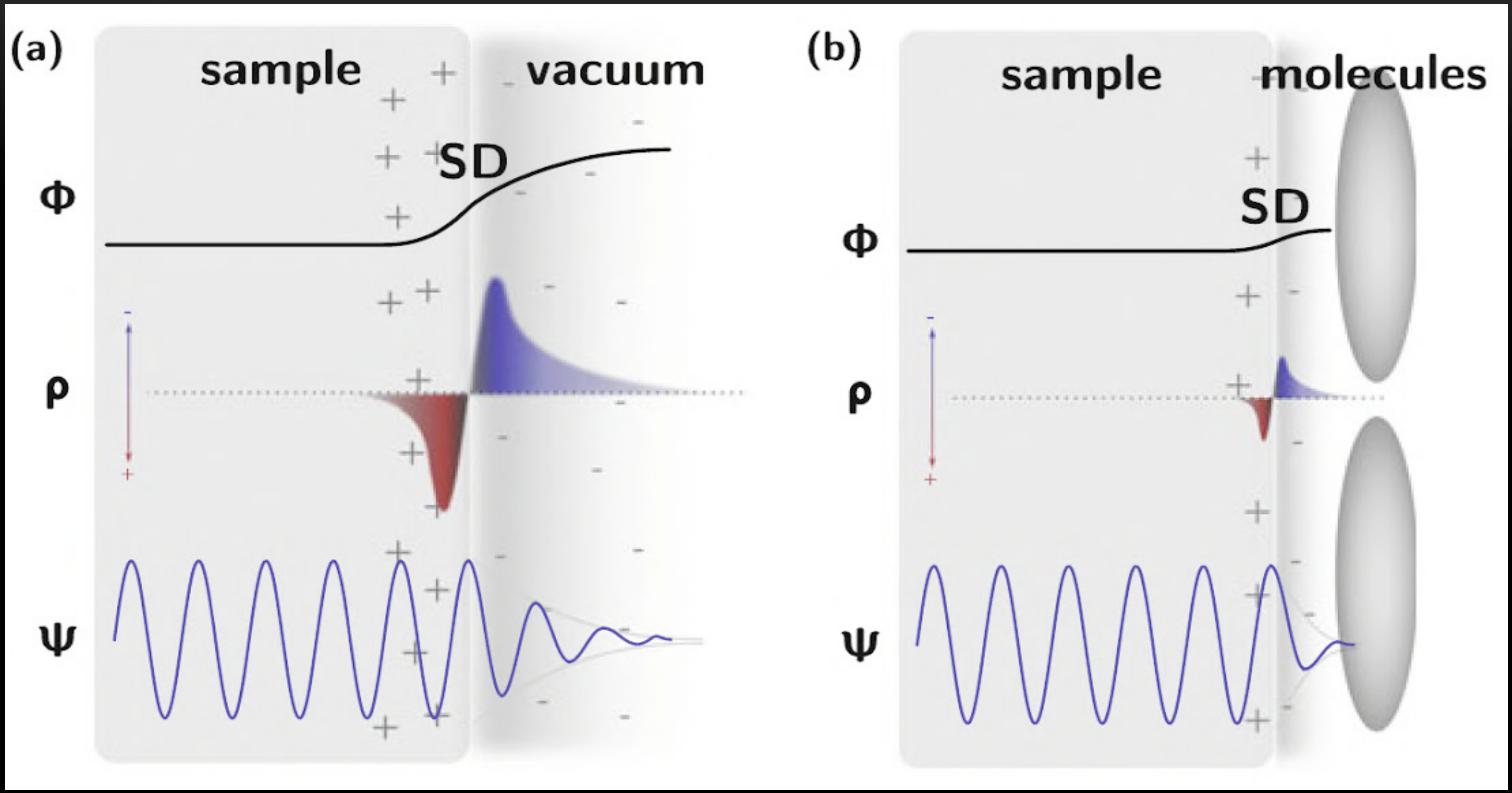

The spill out of the electronic wave function (a) is changed by the physisorbed molecules (b). This effect can be considered as a change of the surface dipole.

R. Schlesinger, Energy-Level Control at Hybrid Inorganic/Organic Semiconductor Interfaces, Springer Theses 2017.

SUMMARY

- Infrared plasmonics and material quality :

$$\omega_{\text{rad}} = \omega_{\tau}$$

- SEIRA of a single dust nanoparticle

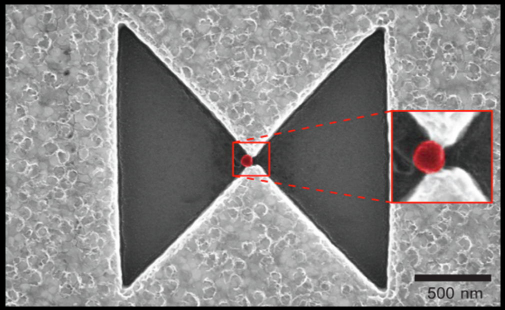

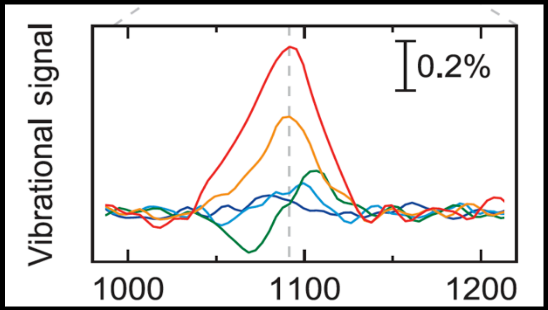

- Low-dimensional plasmonic structures... for adsorption studies: Charge transfer, resitivity change, push back effect

Acknowledgement

Dr. S. Beck, M .Tzschoppe, C. Ulrich, Dr. C. Huck, Dr. J. Vogt , P. Krebsbach, S. Hillebrandt, V. Rohnacher, Dr. M. Sendner

DEPARTMENT OF PHYSICS AND ASTRONOMY

HGSFP

FOR 1700

Deutsche Forschungsgemeinschaft DFG

INNOVATION LAB thinking works

ANKA

INVENTED IN GERMANY

GEFÖRDERT VOM Bundesministerium für Bildung und Forschung

SOLEIL SYNCHROTRON

SFB 1249